Univerza v Mariboru
Fakulteta za energetiko

Journal of ENERGY TECHNOLOGY

Volume 5 / Issue 1
FEBRUARY 2012
www.fe.uni-mb.si/si/jet.html

JOURNAL OF ENERGY TECHNOLOGY

VOLUME 5 / Issue 1

Revija Journal of Energy Technology (JET) je indeksirana v naslednjih bazah: INSPEC©, Cambridge Scientific Abstracts: Abstracts in New Technologies and Engineering (CSA ANTE), ProQuest's Technology Research Database.

The Journal of Energy Technology (JET) is indexed and abstracted in the following databases: INSPEC©, Cambridge Scientific Abstracts: Abstracts in New Technologies and Engineering (CSA ANTE), ProQuest's Technology Research Database.

JOURNAL OF ENERGY TECHNOLOGY

Izhajanje revije / PUBLISHING

Revija izhaja štirikrat letno v nakladi 150 izvodov. Članki so dostopni na spletni strani revije - www.fe.uni-mb.si/si/jet.html.

The journal is published four times a year. Articles are available at the journal's home page - www.fe.uni-mb.si/si/jet.html.

Lektoriranje / LANGUAGE EDITING

Terry T. JACKSON

Oblikovanje in tisk / DESIGN AND PRINT

Vizualne komunikacije comTEC d.o.o.

Oblikovanje revije in znaka revije / JOURNAL AND LOGO DESIGN

Andrej PREDIN

Revija JET je sofinancirana s strani Javne agencije za knjigo Republike Slovenije.

The Journal of Energy Technology is co-financed by the Slovenian Book Agency.

»Manj je več« tudi na področju vetrnih turbin

Današnje komercialne izvedbe vetrnih turbin s horizontalno osjo postajajo vse večjih dimenzij in še vedno izkoriščajo slabih 50% razpoložljivega vetrnega energetskega potenciala (Betz-ova limita – 0,593). Rotor takšnih vetrnih turbin se prosto vrti v toku zraka (vetra) tako, da del le tega odklanja iz rotorskih lopat v radialni smeri – tvori se torej nek »tokovni lijak«, pri katerem se del vetra izgublja oz. preusmerja mimo rotorskih lopat. Znano je, da se fluidni tok odkloni mimo ovire, ki jo v tem predstavlja vrteči se rotor z lopatami, ki tvori nekakšen rotirajoči disk. Rezultat tega dejstva je, da morajo za povečanje energetskega izplena naraščati dimenzije rotorja oz. rotorskih lopatic, višati se mora nosilni stolp, kar pomeni, da celotna konstrukcija postaja vedno bolj občutljiva, še posebej v primeru velikih hitrosti vetra. Zaradi obremenitev se mora rotor vrteti z relativno nizkim številom vrtljajev. Zato je nemalo krat potreben prenos oz. sprememba števila vrtljajev med rotorjem vetrnice in rotorjem električnega generatorja. V tem primeru nastajajo dodatne izgube v prenosih – reduktorjih. Res je, da so sodobni generatorji prirejeni za obratovanje z nizkim številom vrtljajev, tako da se ta pomanjkljivost že odpravlja.

V zadnjem času tudi na področje vetrnih turbin prihaja znan rek iz avtomobilske industrije (manj je več), ki z novimi manjšimi motorji z notranjim zgorevanjem dosegajo večje moči ob hkratnem čistejšem izpuhu, torej z manj obremenilnega vpliva na okolje. Tovrstne nove vetrne turbine so večinoma oplaščene z difuzorjem, ki dodatno niža tlak toka za rotorjem. Na ta način se dosega večja tlačna razlika, pred in za rotorjem, in s tem seveda večja moč. Pri proizvajalcu »FloDesign« navajajo, da lahko izkoriščajo 3- do 4-krat večji izplen vetrnega energetskega potenciala s svojo obliko turbine, ki je oplaščena in ima lopatični vodilnik pred vstopom na rotorske lopate, ki jih je po številu več. Zaradi manjših premerov rotorja (dimenzije) se lahko le-ta vrti z višjim številom vrtljajev brez bojazni glede preobremenitve (loma) materiala.

Oplaščenje (vodilnik) pa hkrati služi kot zvočna izolacija v radialni smeri. Vodilnik (difuzor) so pri tem proizvajalcu tudi inovativno skrajšali v aksialni smeri, kar je seveda zelo zaželeno predvsem z vidika teže in skupnih dimenzij takšne vetrne turbine. Razdeljen je na dva dela v aksialni smeri. Pri tem oblikovanju vodilnika so izkoristili dejstvo, da v kolikor se srečujeta dva toka, različna po smeri in hitrosti, se tvori vrtinec v tokovni sledi in tako navidezno

podaljšuje difuzorski efekt vodilnika, s čimer se še dodatno znižuje tlak za rotorjem in s tem veča tlačna razlika, ki jo lahko energetsko predela rotor.

Zaradi manjših dimenzij celotne izvedbe se problem transporta na mesto postavitve bistveno zniža, saj je namesto večih velikih tovornjakov potreben en sam. To so dosegli s tem, da vetrnico v razstavljenemu stanju naložijo na tovornjak.

Naslednja velika prednost oplaščenih vetrnic manjših dimenzij je tudi v tem, da zaradi manjše skupne teže potrebujejo lažji steber. Znotraj polja, kjer izkoriščamo vetrni potencial, lahko zato postavimo več vetrnic, ker so le-te zaradi manjših dimenzij lahko bližje druga drugi in druga za drugo (manjša vetrna oz. tokovna sled). Klasične vetrnice potrebujejo minimalni razmik okrog 10 premerov rotorja, pri teh oplaščenih je dovolj že 3 premere in to – manjšega premera nove oblike vetrnice. Zaradi oplaščenja se znižuje tudi obratovalni hrup takšnih vetrnic, kar dodatno omogoča, da jih lahko postavljamo tudi bližje urbanim okoljem, saj so manj moteče od klasičnih. Velika prednost je tudi v dejstvu, da lahko zaradi manjših dimenzij obratujejo pri višjih hitrostih vetra, pri katerih je treba klasične vetrnice že zaustaviti (parkirati). Rotorske lopate niso več samo konzolno vpete na pesto rotorja kot pri klasičnih izvedbah, ampak so vpete z dveh strani – tako na pestu kot na zunanji (pokrovni) strani rotorja, oz. na vrhu lopatic. Takšno vpetje lopatic pa omogoča večjo togost samega rotorja in s tem tudi večjo obratovalno varnost tudi pri velikih – orkanskih vetrovih.

Naslednji predstavnik novih vetrnih turbin, podjetje WindTamer, je svojo vetrnico postavilo na istih fizikalnih osnovah, z drugačno rešitvijo difuzorja oz. vodilnika okrog rotorskih lopat. Opuščen je tudi lopatični vodilnik pred rotorjem.

Zelo zanimiv koncept, ki ne sodi med oplaščene izvedbe, pa je vendarle manjših dimenzij, je koncept podjetja Gedayc. Njihova vetrnica bazira na popolnoma drugačni – inovativni geometriji rotorja oz. rotorskih lopatic vetrnice. Izkoristili so dejstvo, da so najvišji energetski doprinosi na večjih premerih in manj v središču vetrnice, kjer je praviloma postavljen generator. Lopate vetrnice so oblikovane tako, da koristijo tok vetra na maksimalnih premerih rotorja vetrnice. Lopate so zato vpete v obroč, kar povečuje celotno togost izvedbe in omogoča obratovanje tudi pri višjih hitrostih vetra.

Predstavljeni koncepti potrjujejo dejstvo postavljeno v naslovu, da je manj več. Enako kot v avtomobilski industriji pri proizvodnji sodobnih motorjev z notranjim zgorevanjem, kjer so uspeli z nižjimi gibnimi prostorninami doseči večjo moč, oz. boljši izkoristek in ob tem še nižje izpuste škodljivih plinov v okolje. Tudi pri predstavljenih konceptih novih, manjših vetrnicah lahko ugotovimo nižji vpliv na okolje, saj so manjše, tišje in energetsko bolj učinkovite od današnjih klasičnih izvedb. Tudi vetrnice z vertikalno postavljeno osjo vrtenja gredo v razvoju v to smer.

'Less is more' with wind turbines

Today's commercial implementation of wind turbines with horizontal axes have larger dimensions and still obtain about 50% of the available wind energy potential (Betz's limit: 0.593). Such a wind turbine rotor rotates in a free stream of air (wind). Part of the approaching air stream is diverted before the rotor blades in the radial direction. The 'funnel flow' shape is thus created. The reason for this is the well-known fluid flow property in

which the fluid flow that approaches the barrier is diverted even before the barrier. This is the reason part of the approaching airflow is diverted in a radial direction and does not pass through the rotor blades. The result of that flow is seen in increased energy loss. To avoid this energy loss, the dimensions of the rotor and rotor blades must be increased, as well as the dimensions of towers. This means that the whole structure is becoming more sensitive, especially in the case of large wind speeds. Due to load, the rotor is rotated at a relatively low speed; therefore a rotation speed transfer (change) between the turbine rotor shaft and the rotor shaft of electric generator is needed. In this case, the additional transfer loss results in common energy lost due to gearbox losses. Nevertheless, modern electric generators are designed and developed for operations at low speeds, which means that gearboxes are not needed.

It has recently been shown that 'less is more' (the famous saying of the automotive industry) holds true for wind turbines. In automobiles, smaller internal combustion engines achieve significant power with cleaner exhausts. Similar effects are achieved in new wind turbines, which are generally coated with a diffuser, which further reduces the pressure-flow across the wind turbine rotor. In this way, a larger pressure difference appears before and after the rotor that results in a power increase. The manufacturer FloDesign states that in this way three to four times higher energy production can be achieved with its type wind turbines. Its turbine has the vane cascade before entering the rotor blades. The number of blades is larger compared with a conventional horizontal axes wind turbine (HAWT). Due to the smaller diameter rotor (dimensions) of the wind turbine, the rotor can rotate with a higher speed without a fear of overloading (fracture) of the material.

The guiding diffuser around the wind turbine rotor blades also serves as sound barrier in the radial direction. The diffuser is shortened in an innovative way in the axial direction, which is of course highly desirable especially in terms of total weight and dimensions of such a wind turbine. The diffuser is divided into two parts in the axial direction. With this design, the fact that when two flows with different direction and velocities meet a flow vortex is formed is used. In this way, the flow current track appears and artificially extends the diffuser effect of the flow guiding in order to further reduce pressure after the rotor, thereby increasing the pressure difference that increase the energy that can be achieved.

Due to small size of the turbine, the problems of transportation to the site are greatly reduced, because only one truck is required instead of several.

The next great advantage of small wind turbines is also in the fact that due to the lower total weight the tower needed is smaller. Inside the flow field, where we use the potential of wind, we can put more wind turbines closer each other because of their smaller dimensions. Conventional wind turbines require a minimum spacing about 10 rotor diameters in the flow direction, while new smaller turbines needs only a three-diameter space between each other in the flow direction. Because of the wind turbine coating, the operating noise of such wind turbines is reduced. This fact allows use closer to the urban environment; they are less intrusive than conventional turbines. The great advantage is in the fact that, due to their smaller dimensions, they can operate at higher wind speeds, at which the classic windmills have to stop (park). Rotor blades are not only cantilever mounted on the rotor hub as with the traditional designs, but they are mounted on both sides (both at the hub and at tip) at the top of the blade. Such suspension blades, which allow a higher stiffness of the rotor itself, thus also increase operational safety even in strong winds.

A representative of the new wind turbine company, WindTamer, has presented his turbine developed on the same physical basis of the alternative treatment of the diffuser around the rotor blades. At the same time, guide vanes before the cascade of rotor blades have been abandoned.

The next highly interesting concept is not included in the coated wind turbine concepts, but it is of small dimensions. The company Gedayc has wind turbines based on a completely different and innovative geometry of the rotor or rotor blades of wind turbines. The advantage can be found in the highest energy yield at a larger diameter and less in the centre of wind turbine rotor, where the generator is normally positioned. Wind turbine rotor blades are designed to benefit from the flow of wind at maximum rotor diameter. Blades are therefore trapped in the ring, which increases the overall stiffness performance of the entire rotor structure and allows operation at higher wind speeds.

The new concepts presented confirm that less is indeed more, in both the automotive and wind turbine industries. Also, these new small wind turbines have a lower impact on the environment, because they are smaller, quieter and more energy efficient than today's classic turbines. The new concept is also reflected in the development of wind turbine with vertical axis rotation.

Krško, February, 2012

Andrej Predin

Table of Contents /
Kazalo

JET Volume 5 (2012), p.p. 13–26

Issue 1, February 2012

http://www.fe.uni-mb.si/si/jet.html

DIGITAL METER OF REACTIVITY FOR USE DURING ZERO-POWER PHYSICS TESTS AT THE KRŠKO NPP

UPORABA DIGITALNEGA MERILNIKA REAKTIVNOSTI PRI ZAGONSKIH TESTIH NA NIČELNI MOČI V NE KRŠKO

Igor Lengar[ℜ], Andrej Trkov, Marjan Kromar, Luka Snoj

Keywords: Digital reactivity meter, Zero-Power Physics Tests, Start-up tests, Point Kinetics Equation, NPP

Abstract

A part of nuclear fuel is exchanged during an outage in a NPP, with an influence on the reactor characteristics. The parameters of the new reactor core are determined with nuclear design calculations and must be experimentally verified during reactor start up. For accurate determination of these characteristics, a device for measuring reactivity is necessary.

The key tool for the performance of zero-power physics (start-up) tests at the Krško NPP is the digital meter of reactivity (DMR), developed in the 1980s at the Reactor Physics division of the Jožef Stefan Institute, in Ljubljana, Slovenia. It was the first digital device to be used within a wide range of operating conditions for the measuring of reactivity. These conditions also include measuring reactivity in a deeply subcritical reactor, which enables the DMR to determine the integral and differential worth of control banks during their insertion into the core. This new method was named 'the rod-insertion method'.

[ℜ] Corresponding author: Igor Lengar, PhD., Tel.: +386 1 588 5253, Fax: +386 1 588 5454,
Mailing address: Jozef Stefan Institute, Reactor Physics Division, Jamova 39, SI-1000 Ljubljana, Slovenia
E-mail address: igor.lengar@ijs.si

The performance and development of the DMR is presented in this paper. Its unique characteristics are described with the example of the rod insertion method. Also presented are examples of measurements during the start-up physics tests at the Krško NPP.

Povzetek

V nuklearnih elektrarnah med remontom zamenjajo del jedrskega goriva, s čemer se spremenijo karakteristike reaktorja. Te se predhodno določijo s projektnimi izračuni, pred zagonom reaktorja pa jih je potrebno preveriti z meritvami. Za ustrezno preveritev karakteristik reaktorja je potrebna naprava, s katero je možno meriti reaktivnost.

Ključna naprava pri izvajanju zagonskih testov v jedrski elektrarni v Krškem je Digitalni Merilnik Reaktivnosti (DMR), ki je bil v 80ih letih razvit na Odseku za reaktorsko fiziko Instituta Jožef Stefan. DMR je bil prva digitalna naprava, ki je lahko merila reaktivnosti v širokem delovnem območju, vključno z meritvami v globoko podkritičnem reaktorju. Ta lastnost omogoča DMR določitev integralnih in diferencialnih vrednosti kontrolnih svežnjev med njihovo vstavitvijo v sredico. Nova metoda določanja vrednosti kontrolnih svežnjev je bila poimenovana metoda vstavitve (rod-insertion method).

V članku je predstavljen razvoj in delovanje DMR. Njegove edinstvene karakteristike so predstavljene na primeru uporabe pri metodi vstavitve. Podani so tudi primeri meritev med zagonskimi testi v NE Krško.

1 INTRODUCTION

One of the most important parameters of a reactor during operation is the criticality, k, or the connected reactivity, ρ. They are a measure of the balance of neutrons in the system and through this of the change of reactor power (or neutron flux) with time. The reactivity is defined as in [1]

$$k = \frac{n_N}{n_{N-1}} \tag{1.1}$$

where n_N is the number of neutrons in a generation and n_{N-1} is the number of neutrons in the preceding generation. The reactivity is defined as

$$\rho = \frac{k-1}{k} \tag{1.2}$$

If $\rho>0$ the flux increases, for $\rho<0$ the flux decreases and is stable in the case of $\rho=0$. The reactivity of a reactor is affected by several factors, including the insertion of control rods, the concentration of boron in cooling water or the change in temperature, etc. The first two ways are usually used for reactivity control.

In a simple approximation, the flux in a reactor behaves exponentially over time with a specific time constant, T – the period. This is valid for small absolute reactivity; in case there are no temperature feedback effects, no significant independent source of neutrons, and after some

time has passed from the last transient (see Section 2). This exponential behaviour introduces a possible, and very common, way of measuring reactivity, i.e. by observing the time dependence of the flux, extracting its doubling time and then calculating the reactivity.

Such a method for determining reactivity has, however, several limitations: it cannot be used during transients, each measurement is very time consuming, etc. For this purpose, in the 1970s and 1980s, devices called 'reactivity meters' were developed by different groups, [2,3], based on solving the reactor point kinetics diffusion equations for the neutron flux, as described in Section 2. Most of the early devices were analogue computers, [3], requiring sensitive potentiometer settings, and the maintenance of several analogue components. The accuracy of the results of these devices was moderate, but they were still superior to the previously described period measurements.

The researchers of the reactor physics division were among the first to develop a digital version of the reactivity meter, based on processing the signal by a computer. The device was called a Digital Meter of Reactivity, or DMR. It is composed of a programmable picoammeter, AD/DA converters, a PC computer and the accompanying software. From the start, the DMR was superior to other similar devices, especially for the measurements of control rod worth using the rod-insertion method (see Section 3). The theoretical basis and the performance of the DMR are described in this paper. Examples of measurements at the Krško NPP are presented.

2 THEORETICAL BACKGROUND

The time-dependent point kinetics equations, [1], with *I* groups of delayed neutron precursors are:

$$\frac{dP(t)}{dt} = \frac{\rho(t)-\beta}{\Lambda} P(t) + \sum_{i=1}^{I} \lambda_i C_i(t) + Q(t) \tag{2.1}$$

$$\frac{dC_i(t)}{dt} = \frac{\beta_i}{\Lambda} P(t) + \lambda_i C_i(t), \quad i = 1,\ldots,I \tag{2.2}$$

where

$P(t)$ is the neutron flux,
$\rho(t)$ is the reactivity,
$C_i(t)$ is the number density of the i-th group of delayed neutron precursors,
β_i is the effective delayed neutron fraction of the i-th delayed neutron group,
λ_i is the decay constant of the i-th group of delayed neutrons,
β is the effective total delayed neutron fraction (summed over all β_i),
Λ is the prompt neutron lifetime,
Q is the neutron source term.

All these quantities are defined as weighted space averages. When the neutron source term, Q, is neglected, the system of equations is homogeneous. If reactivity, ρ, is constant, a solution of the form

---

$$P \alpha e^{t/T} \tag{2.3}$$

may be assumed where T is a parameter. Since the system of equations for P and C_i is homogeneous, a solution exists only when the determinant is zero. The characteristic polynomial for the determinant is the Inhour equation

$$\rho = \frac{\Lambda}{T} + \sum_{i=1}^{N} \frac{\beta_i}{1+\lambda_i T} \tag{2.4}$$

This is an algebraic equation for T of order N+1. The Inhour equation can be used to determine ρ if parameters Λ, β_i, λ_i are available and the source term, Q, is negligible. The asymptotic period, T_l, can be measured from the asymptotic flux behaviour. This is the most straightforward way to measure the reactivity of a reactor and was often used, especially in the past, [1]. The neutron kinetics parameters must be determined by independent measurements or taken from the literature.

Most of the reactivity meters, analogue or digital, used this simplified equation (2.4) as the basis for reactivity calculation, [3]. The DMR developed at the Jožef Stefan Institute is, however, based on a less simplified version of the diffusion equations (2.3) and (2.4) including the source term. It calculates the reactivity without relying on the asymptotic flux behaviour. Equations (2.1) and (2.2) are integrated analytically. Assuming that the neutron flux was steady until time $t = 0$, substituting equations (2.4) into equation (2.3), and after rearrangement, the inverse point kinetics equation is obtained:

$$\rho(t) = \frac{\Lambda}{P(t)} \cdot \frac{dP}{dt} + \sum_{i=1}^{I} \frac{\beta_i}{P(t)} e^{-\lambda_i t} \int_0^t \frac{dP}{dt'} e^{-\lambda_i t'} dt' - \Lambda \frac{Q(t)}{P(t)} \tag{2.5}$$

This equation is the basis for the calculation of the reactivity by the digital reactivity meter. In the DMR, the neutron flux signal, P, is sampled at certain time intervals. This information is processed by the reactivity meter software. Numerical integration is performed to determine the reactivity, ρ. Details on the neutron signal processing and the algorithms for numerical integration are described in reference, [4], and are beyond the scope of this work.

The theoretical basis for the Digital Meter of Reactivity is formed by equation (2.5). In order to make a device that can be used in practice, several problems have to be solved, among the most important being the noise filtration, background elimination, neutron flux redistribution effects during control rod movement in the reactor, etc. In the continuation, the solutions used by the DMR for the listed problems are described and its operation is demonstrated with measurements during the Krško NPP zero-power physics (start-up) tests after refuelling.

3 DIGITAL METER OF REACTIVITY OPERATION

The input parameters for the DMR are the current signal, I, which is proportional to the neutron flux (and reactor power), and obtained from ionization cell(s) or another detector, and the voltage signal representing the temperature of the core, T. The output is the value for the

reactivity, ρ, presented in real-time. Before the start of measurements, nuclear constants for the specific reactor to be measured are also needed as input. The final version of the DMR at the Jožef Stefan Institute, completed in 1994, has the identification number DMR-043. Its schematic is presented in Figure 1.

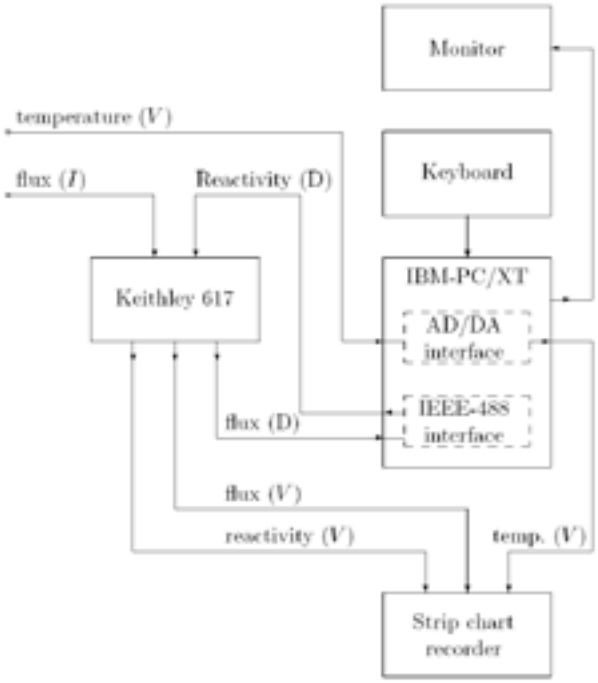

Figure 1: *Block diagram representing the digital reactivity meter DMR-043 hardware connections. Symbol (D) represents a digital signal, symbol (V) represents an analogue voltage signal and symbol (I) represents an analogue current signal*

As noted, equation (2.5) is used as the basis for the numerical integration in the DMR, but several practical problems in connection with signal processing have to be solved in order to produce a device that can be used and that produces meaningful results. The strength of the DMR-043 in comparison to other reactivity meters is its capability to give correct results for ρ in a very broad range of reactor operating conditions, which include:

- operation at low power where the neutron flux is dominated by the source term (Q in equation (2.5)),
- in a deeply subcritical reactor,
- during measurements of transients,
- during redistribution effects of the neutron due to control bank movements.

Special solutions had to be implemented in the DMR-043 in order to cover the described cases (among others). Some of the problems are listed in the continuation and are demonstrated with the rod-in measurement method (described in Section 4). Because a detailed analysis is beyond the scope of this work and can be found in [4], only a general description is presented.

3.1 DMR-043 algorithms

3.1.1 Signal smoothing

One of the main concerns is how to minimize the effect of random noise on the neutron flux signal. To filter out the noise and improve the stability of the reactivity meter, three levels of signal smoothing are applied. The primary smoothing is performed inside the Keithley electrometer through the integrator circuit. The secondary smoothing allows further filtering of the signal to remove low frequency oscillations in the signal. It is defined by the signal sampling technique, which makes full use of the Keithley electrometer special features. Tertiary smoothing is performed by the DMR-043 software and is related to the algorithm for calculating the recurrence relation, by which the equation (2.5) is numerically solved.

3.1.2 Error analyses

Much care is devoted also to identification of possible error sources and their treatment. The major sources of errors dealt with by the DMR are presented.

Error in the signal – The signal is corrupted with background radiation, mainly consisting of gamma rays from fission and activation products. This background is rather stable and introduces an addition to the signal. The problem is treated by subtracting the background from the signal. Several methods were developed in order to obtain the best estimate for this background signal. It is evaluated in a deeply subcritical core before reactor start-up. Another method is determination during the rod-insertion method, when the measured control rod is fully inserted (Section 4).

Corrections due to the neutron source – The neutron source term, the last term in equation (2.5), becomes important when the reactor power is low. Its value is difficult to measure. DMR-043 estimates the value of the source with an algorithm during the approach to criticality, i.e. when the state of the reactor is changed from a deeply subcritical to a slightly subcritical state.

Flux redistribution effects – The neutron flux redistribution during the reactivity measurements affects the results through the effective change in the delayed neutron data and especially through the ratio of the measured and the true core average neutron flux. Equation (2.5) constrains the approximation of reactor point kinetics, i.e. for the average neutron flux in the core. The results are accurate if the signal, measured with the ionization cell, is proportional to the average flux. This would be true if the flux distribution in the core was constant with time. During control rod movement, the flux is, however, redistributed and the ratio between the average flux and the measured flux changes. DMR-043 takes this into account by assignment of a special flux redistribution factor, which is calculated in advance for the particular reactor configuration and control bank.

Error in nuclear constants – The inadequate values of nuclear constants Λ, λ_i, β_i are reflected in the incorrect value of reactivity. The constants are calculated for the specific reactor and core loading and input into the DMR before its usage.

---

4 THE ROD-INSERTION METHOD WITH USE OF THE DMR

Most of the DMR-043 special features and solutions, which make it so unique, can be described with the rod worth measurement with the rod-insertion method. This method is particularly convenient, because it is very quick and simple to perform. The time needed for the measurement of one control bank in the Krško NPP has decreased with the use of this method from a few hours to a few minutes, with regards to the previously used methods, [6].

4.1 Rod worth measurements

After each refuelling in a NPP, post-refuelling nuclear core design check tests are performed in order to prove that the reactor core characteristics are as designed. At the Krško NPP, the most important tests, which are performed before going to power, include boron endpoint determination, isothermal temperature coefficient determination and control bank worth measurement at zero power. Before the application of the DMR, the great majority of time required for the tests was needed for bank worth measurements. Four different methods were used: dilution/boration, rod swap, rod swap with a 'swinging' reference bank and subsequently rod-insertion, [7]. The first three methods are based on differential rod worth measurement while maintaining the reactor at an almost critical level: it means that small reactivity change, introduced into the core by the bank being measured is compensated either by dilution/boration or by a reference bank.

4.2 Rod-insertion method

The rod insertion method is based on a different approach: bank-worth measurement is performed while the core goes into a subcritical region; no reactivity compensation is required. The principle of the rod-insertion method is to start from a critical reactor, operating at low power, and to measure the time-dependent reactivity change while a control rod is inserted into the core. Unlike in the rod-drop method, [1], the measured control rod is inserted with the Control Rod Drive Mechanism (CRDM), at normal speed. By analysing the flux trace using the DMR, not only the total rod worth but also the differential and the integral control rod worth curves are obtained.

During the rod-insertion measurement, the flux may drop by several orders of magnitude, because the reactor has become deeply subcritical. Therefore, the DMR with the high-quality electrometer is required for monitoring the neutron flux and for the data analysis. The stored data are then analysed off-line.

4.2.1 Steps during the rod-insertion method

First the 'raw' measured reactivity is obtained, which is calculated using equation (2.5). Appropriate Fourier smoothing is applied on the signal in order to eliminate neutron noise and noise due to electronics.

The next step is the **elimination of the background**, which can, in this case, not be ignored. The background can be evaluated accurately from the data collected during the measurement itself. A value for the background is selected such that the calculated reactivity is constant after the insertion. This can be done conveniently with a least-squares procedure.

The next correction that has to be applied is the **flux redistribution correction** due to control bank insertion. During the insertion of a control bank into the core, the distribution of the neutron flux is altered. This generally results in a larger signal change in the case of the insertion of a control bank on the periphery and closer to the ionization cells than in the case of insertion of a control bank in the centre, although the reactor power change is equal in both cases. Another consequence of the flux redistribution is that the point kinetics approximation (Equations (2.3) to (2.5)), in which the time and space separability of the neutron flux is assumed, is no longer valid. The problem is solved by assigning a correction factor to each control bank. This factor is calculated in advance within the standard core design calculations.

The **neutron source** is determined separately. Neglecting it would produce a slight overshoot in reactivity (10–15 pcm) during rod withdrawal when the original (critical) configuration is regained. This is removed entirely by specifying a neutron source term.

All of the described corrections have to be taken into account in order to obtain correct results. The described procedure is illustrated in the following figures with the measurement of the differential curve for the Control Bank C of the Krško NPP during the start-up tests after refuelling in 1989, [5, 8].

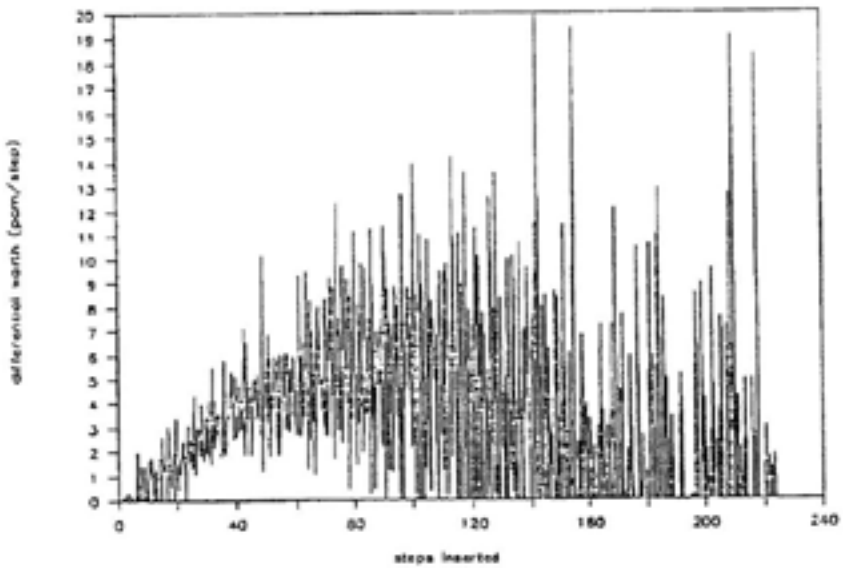

Figure 2: *Differential reactivity curve, control bank C of the Krško NPP in 1989, calculated from raw data and uncorrected for background*

As can be seen from Figure 2, the raw data cannot be used in the case of the rod-insertion method, although it gives good results if the reactor is close to critical and the flux is larger. This is also frequently used by other reactivity meters. In the case of the rod-insertion, additional smoothing of the raw data is necessary with the use of a Fast Fourier Transform algorithm. The improvement is clearly visible on Figure 3.

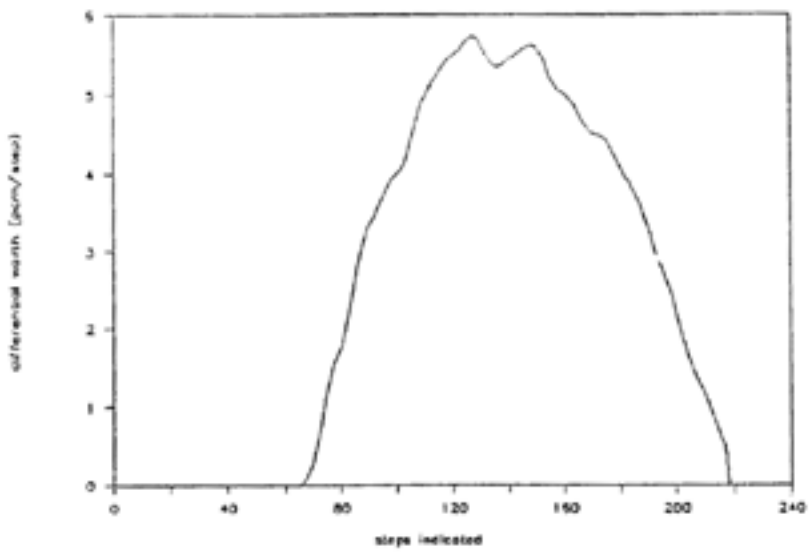

Figure 3: *Differential reactivity curve, control bank C of the Krško NPP in 1989, data smoothed with the Fast Fourier Transform, uncorrected for background*

The next step is the removal of the background and the insertion of the correct source strength *Q*. The exact procedure is beyond the scope of this work and described elsewhere, [5]. The results of the background removal algorithms can be seen on Figure 4.

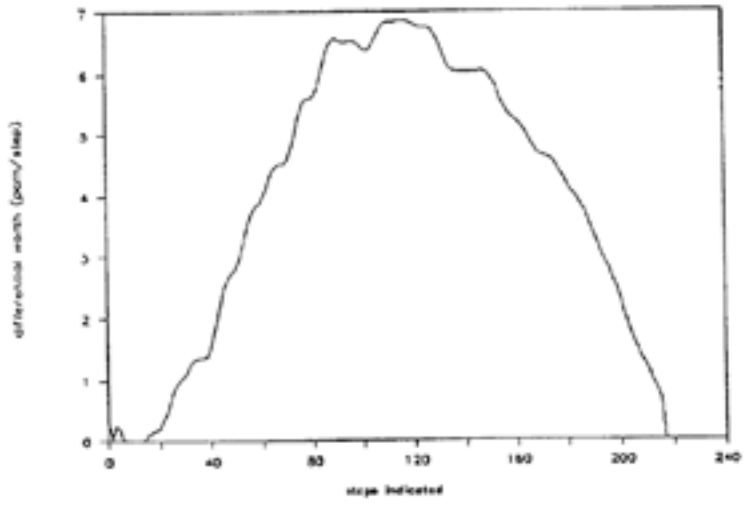

Figure 4: *Differential reactivity curve, control bank C of the Krško NPP in 1989, data corrected for background, not corrected for radial redistribution*

As the final correction, the flux redistribution effect is taken into account (Section 3). The final results of the rod-insertion method are the integral and differential bank-worths. The correctness of the method is illustrated with a comparison of the results, obtained from two approaches: with the rod-insertion method and with the previously used method of

---

dilution/boration. Both methods are used for one of the control or shut-down banks during the start-up physics tests in the Krško NPP. The comparison is made on hand of the cycle 25 data, performed in November 2010, when the shut-down bank SA was measured with both approaches. A comparison of the methods and with the design calculated value is presented in Figure 6 for the differential curves and in Figure 7 for the integral curve, [9].

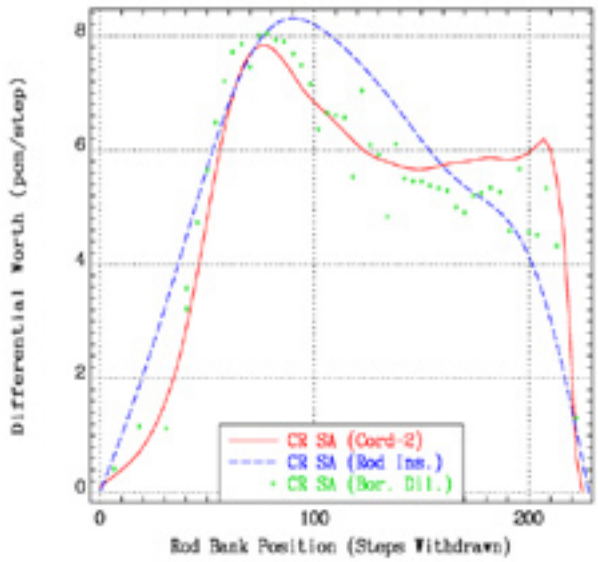

Figure 5: *Comparison of the differential worth for shutdown bank SA: Boron Dilution, rod-insertion method and design predicted curve (IJS design). Data from start-up physics tests for cycle 25 of NEK, November 2010*

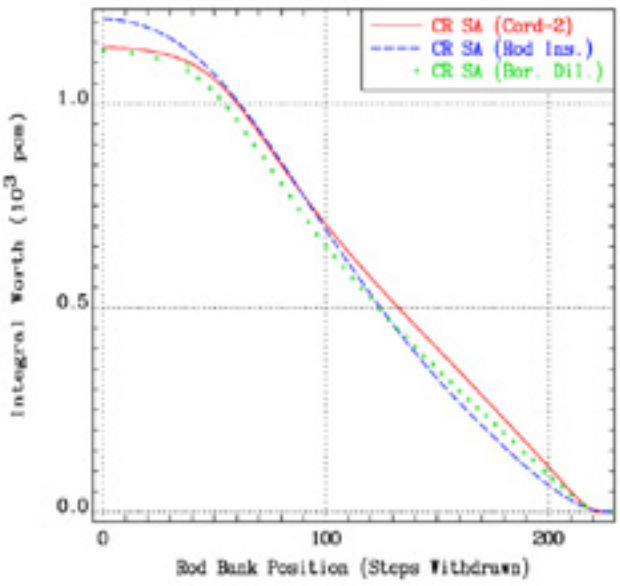

Figure 6: *Comparison of the integral worth for shutdown bank SA: Boron Dilution, rod-insertion method and design predicted curve (IJS design). Data from start-up physics tests for cycle 25 of NEK, November 2010*

4.2.2 Success of the method

The rod-insertion method was developed for applications in pressurized water power reactors. It was first tested at the Krško plant in 1987, [8], and at the Kernkraftwerk Obrigheim in 1988, [10]. It was then further improved, and since 1989 it has been the principal method for control rod worth measurements during the physics start-up tests after refuelling at the Krško plant. Shortly after that the method was adopted and verified independently under the name the 'dynamic method' by Chao et al., [9], at Westinghouse and Wisconsin Electric. The rod insertion method has also been used at research reactors, [7, 12]. Next to the reduction of measurement time, the great benefit of the rod insertion method in the case of power plants is also that the amount of waste coolant is drastically reduced since no dilution or boration is required.

Table 1 presents the time required for measuring the worth of all six control and shut-down banks at the Krško NPP, using three different methods that were used in the past at NEK. Included are data about the waste coolant consumption, [5].

Table 1: *Inter-comparison of merits for three rod worth measuring methods. Values are approximate and reflect the state for Krško NPP 1989 start-up, [5]*

method	time required (hours)	total change in boron concentration (ppm)	waste water (m3)	waste boron (m3)
boron exchange	48	490	45	9
rod swap	12	166	16	4.5
rod-insertion	1–2	0	0	0

Table 1 clearly shows the rod-insertion method's advantages to the boron exchange method, as well as to rod swap method regarding both time and waste coolant production. The rod-insertion method was approved by the Slovenian regulatory body, and since 1989 has been used as the main measuring method for control bank worth during the Krško NPP start-up tests. NEK is the first power plant in the world in which the rod-insertion method was used and it shortened the time required for the start-up physics tests, from several days to 12 hours, resulting in considerable savings of time and money. The quality of the method can also be deduced from the fact that it was latter adopted by Westinghouse for start-up measurements, [11], and is today used in several power-plants around the world.

5 MEASUREMENT OF THE TEMPERATURE COEFFICIENT

Perhaps the most important parameter that has to be satisfied at all times during a power reactor operation is the value of the isothermal temperature coefficient (ITC). It is also measured during each start-up test; the DMR device is indispensable for its determination. The temperature coefficient α_{iso} is defined as the change in reactivity with respect to the change of the reactor core temperature and must be negative throughout the cycle. During the measurement of α_{iso}, the temperature of the coolant water is slowly lowered by approximately 2°C within half an hour and then raised again to the initial value. The reactivity is closely monitored. Since the absolute value of the coefficient is usually small at the beginning of each cycle, the accurate DMR has to be used for reactivity recording. The measurement of the ITC during the start-up physics tests for cycle 25 of NEK (November 2010) is presented in Figure 7. A sufficiently precise measurement would be very difficult or impossible to perform with analogue devices.

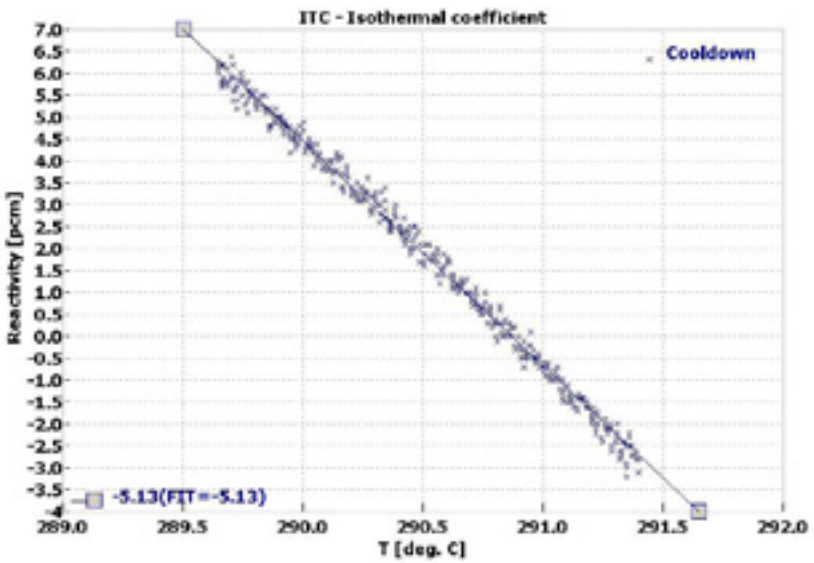

Figure 7: *Isothermal coefficient measurement at NEK; start-up physics tests for cycle 25, November 2010*

The DMR enables very fast evaluation of the data. The results are available right or shortly after the measurement, and the preliminary values for all major parameters are presented before the

---

end or the start-up tests. This is great progress from analogue reactivity computers, with which data reduction and preparation of test reports had been done manually and required much time and labour [3].

6 CONCLUSIONS

A Digital Meter of Reactivity was developed, based on solving the point kinetics equations including the source term. It is composed of a programmable picoammeter, AD/DA converters, a PC computer and the accompanying software. From the start, the DMR was superior to other similar devices, due to its ability to give correct results in a very broad range of reactor operating conditions, including measurements in a deeply subcritical reactor. Special solutions had to be implemented in the DMR in order to cover the broad range of cases.

The rod-insertion method makes full use of the special features available in the DMR. It is used for bank-worth measurements, during which a control bank is inserted into the core with the control rod drive mechanism at normal speed. No reactivity compensation is required; thus, the method is much faster than other available methods. The method has routinely been used during the start-up tests at the Krško NPP since 1989; it shortened the time required for the tests from several days to 12 hours. After the success in NEK, the rod-insertion method was adopted by others and is today used in several power plants around the world.

The DMR is used also for other measurements during start-up tests, e.g. for the isothermal temperature coefficient determination. It enables very fast evaluation of data and the results are available shortly after the measurement.

References

[1] **R. Keepin.:** *Physics of Nuclear Kinetics,* Addison-Wesley, 1965.

[2] **Hoffspiegel, P.; Kaplan, G.; Long, S.; Reum, S.; Rohr, P.:** *Development of the Combustion Engineering Reactivity Analyzer System.,* Proc. Int. Reactor Physics Conf., Jackson Hole, Sept. 18–22, 1988, Suppl., p. S-139.

[3] **Shimazy Y.; Nakano, Y.; Tahara, Y.:** *Development of a Compact Digital Reactivity Meter and a Reactor Physics Data Processor,* Nuclear Technology 77 (1987) 247.

[4] **Trkov, A.:** *Digital Reactivity Meter DMR-043: Part A – Theory and Methods Part B - Users' Manual, Part C - Validation.* Institute Jožef Stefan Report IJS-DP-5238, Ljubljana, April 1990 (original distribution and revisions up to September 2004).

[5] **Glumac, B.; Trkov, A.; Skraba, G.:** *Digital Reactivity Meter DMR- 043 (Rod Insertion Reactivity Computer),* Institute Jožef Stefan, Report IJS-DP-5855, July 1990.

[6] **Trkov, A.; Ravnik, M.; Wirnmer, H.; Glumac, B.; Böck, H.:** *Application of the rod-insertion method for control rod worth measurements in research reactors,* Kerntechnik 60 (1995) 255–261.

[7] **Glumac, B.; Škraba, G.:** Rod Insertion Method for Rod Worth Measurement. Proc. Technical Committee Meeting on Operational Safety Experience of Two-loop Pressurized Water Reactors, Bled, May 30–June 3,1988. IAEA-650 (1989). p. 280–297.

[8] **Glumac, B.:** *Meritev vrednosti kontrolnih svežnjev A in D z metodo vstavitve kontrolnega svežnja v NE Krško v letu 1987.* (Measurement of Control Rod Wort1 of

---

Banks A and D by the Rod-Insertion Method at the Krško NPP in 1987, in Slovene.), Institute Jožef Stefan, Report IJS-DP-5047, Ljubljana, March 1988.

[9] **Lengar, I.; Žerovnik, G.; Trkov, A.; Kromar, M.; Snoj, L.; Žefran, B.:** *Report on the Zero-Power Physics Tests for Cycle 25 of the Krško NPP,* Institute Jožef Stefan, Report IJS-DP-10586, Ljubljana, November 2010.

[10] **Glumac, B.; Kromar, M.:** *Meritev vrednosti kontrolnih in zaustavitvenih svežnjev tlačnovodnega reaktorja z metodo vstavitve.* (Measurement of Control Rod Worth of Control and Shutdown Banks in a Pressurized Water Reactor by the Rod-Insertion Method, in Slovene.), Institute Jožef Stefan, Report IJS-DP-5397, Ljubljana, July 1989.

[11] **Chao, Y A.; Chapman, D. M.; Eaner, M. E; Hill, D. J.; Hoerner, J. A.; Kurtz, P.N.:** *Methodology of the Westinghouse Dynamic Rod Worth Measurement Technique.,*Trans Am. Nucl. Soc. 66 (1992) 479.

[12] **Trkov, A.; Ravnik, M.; Böck, H.; Glumac, B.:** *Reactivity measurements in a close-to-critical TRIGA reactor using a digital reactivity meter,* Kerntechnik 57 (1992) 296–300.

JET Volume 5 (2012), p.p. 27 - 36

Issue 1, February 2012

http://www.fe.uni-mb.si/si/jet.html

SUSTAINABLE CULTURE AND ENERGY USE IN HOTEL RESORTS

TRAJNOSTNA RABA ENERGIJE V HOTELIH

Milan Ambrož[ℜ], Božidar Veljković

Keywords: sustainability, tourism, energy, consumption, behavior, strategy, organizational culture

Abstract

The aim of this study was to investigate the mission of hotels and hotels resorts regarding the development of sustainable tourism. The organizational behaviour regarding the energy consumptions of thirteen hotels from Posavje, and the 47 employees and managers from these hotels participated was examined.

They were questioned with a Likert type questionnaire about the factors that influence their attitudes toward sustainable energy consumption in hotel. Empirical findings of the study show that long-term vision, long-term strategy-oriented behaviour, consensus seeking about energy consumption, and employee involvement are the most important factors of sustainable behaviour. The study opens a new perspective in the research of the emergence of 'green' culture based on energy consumption strategy, innovative governance of waste and waste water and its recycle fire and accident protection, transforming solid waste into new energy, the use of new technology, and the integration of the infrastructure of tourism systems.

Povzetek

Cilj naše študije je bil raziskati vlogo poslanstva skupine hotelov ali hotela pri razvoju trajnostnega turizma. V študiji je sodelovalo 47 zaposlenih v trinajstih hotelih v Posavju. Anketiranci so izrazili svoja stališča do trajnostne rabe energije v hotelu, kjer so zaposleni. Rezultati študije kažejo, da so faktorji dolgoročna vizija, dolgoročno usmerjena strategija, iskanje soglasja pri trajnostni rabi energije in vključenost zaposlenih v proces sprememb ključni pri razvoju »zelene« kulture. Naša študija odpira nove perspektive raziskovanja vedenjskih

[ℜ] Corresponding author: Milan Ambrož, PhD., Tel.: +386 4 280 83 04, Mailing address: B&B izobraževanje in usposabljanje d.o.o., Žagarjeva 27A, SI-4000 Kranj, Slovenia
E-mail address: milan.ambroz@bb-kranj.si

---

vzorcev v organizacijah na področju turizma, ki so usmerjeni k razvoj »zelenih« struktur, ki delujejo po načelih »zelene kulture«. Zelena kultura temelji na vedenju, ki nadzira energijsko strategijo, inovativno upravljanje z odpadki, varovanje pred požarom in pred nesrečami. Poleg tega zelena kultura temelji na uporabi nove tehnologije za varčevanje z energijo in na združevanju infrastrukturnih sistemov v turizmu.

1 INTRODUCTION

Among other resources, the hospitality industry uses a substantial amount of energy in providing comfort and services to its guests. The energy consumption practices of hotels that function as SMEs or as large resorts have surprisingly low-energy efficiency, [9]. While providing significant benefits to local and national economy, the accelerated growth of the hotel industry is a serious threat to natural and socio-cultural environments. To preserve future generations' resources and the quality and attractiveness of tourist destinations, a new sustainable approach is needed.

The tourism industry is growing rapidly and is identified as the leading force in service industry. In Slovenia, tourism contributes significantly to the economy, and there are significant contributions in the Posavje region. The performance of hotel resorts in Slovenia is diminishing due to low performance. Some studies have attempted to link poor performance to the culture of organization, [1-3].

This paper investigates the relationship between organizational culture and energy efficient hotel resorts in the Posavje region. While many studies have emphasised the role of organizational culture, only a few have investigated its effectiveness in the building of sustainable tourism behavior in SMEs, [1-5].

Conceptualizing organizational culture as the attitudes and behavior practices, it is defined as intangible characteristics of organization. Denison, [6], defines organizational culture as a set of values, principles, and norms that drive organization and shape the organization members' views of the internal and external organization context. Denison and Mishra, [1], conceptualize organizational culture along four dimensions that have been shown to relate to organizational effectiveness: involvement, consistency, adaptability, and mission. The learned responses to the problems of internal integration are observed in the traits of involvement and consistency. Survival in the external environment is characterised by adaptability and mission traits; they describe the extent to which SMEs are customer focused and strategically oriented.

Our research shows how organizational culture is linked toward energy consumption effectiveness in tourism hotel resorts, [8]. As awareness of tourism's energy impacts on environments increases, the effectiveness of SMEs in tourism becomes increasingly important. More productive and effective business operations lower costs and improve customer satisfaction and build sustainable behavior.

2 SUSTAINABLE USE OF ENERGY

Demand for energy resulting in the depletion of natural resources is increasing every day. Energy use is becoming a major threat to the world's climate. The sustainability of tourism is part of the answer, because it is argued that tourism, and particularly the recreational part of it, may contribute considerably to the consumption of energy.

Becalli et al., [11], show that tourist attractions such as museums consume less energy than tourist activities such as scenic flights or jet boating. Motorized travel is one of the greatest energy-consuming activities, [12-13]. Research by Budeanu, [14], showed that despite their declared positive attitudes towards sustainable tourism, only a few tourists act accordingly by buying responsible tourism products. They rarely choose environmentally friendly transportation. Their behavior is not responsible, even if they see the negative impact of their behavior on the hosting community. The lack of initiatives to increase customers' attention toward sustainable tourism is evident.

Nevertheless, since the early 1990s, tourism companies have engaged in the development of sustainable tourism. Many hotels participate voluntarily. They mostly use codes of conduct, best environmental practices, eco-labels, and environmental performance indicators, [10]. Some hotels use the measures designed for energy saving and the reduction of CO_2 emissions, [12].

The findings of the Cham and Lam [15] indicate that the existing green measures and devices are inadequate to cope with the increase in pollution emission in hotels in the near future. They believe that the hotel industry should adopt a more proactive approach to reduce electricity usage, and propose the inclusion of environmental reporting in trade journals, [16]. Karagiorgas et al., [22], follow a proactive approach with implemented conditions for the massive application of future renewable energies in the tourism industry.

3 SUSTAINABLE ORGANIZATIONAL BEHAVIOUR

Climate change and other global problems require changes in tourism behavior, especially in the field of energy consumption. Renewable energy, organic food along with a responsible way of life is the concept that should be strongly addressed in the future. In this section, we argue for a complex view of organizational culture and its impact on energy consumption, one which integrates values, knowledge structures, and beliefs, as well as practices, artefacts, rituals, rules for social interactions, and roles that groups develop over time in the pursuit of common goals, [17]. Schein, [18], proposes a more managerial view of organizational culture, i.e. ‘a pattern of shared basic assumptions a group learned during the problem solving processes.

The role of organizational culture is twofold: (1) to integrate individuals into an effective whole, (2) to effectively adapt of the organization to the external environment. These two elements build a base for the sustainable behaviour of an organization. In the case of hotels and hotel resorts, there is a great need to integrate the efforts of all stakeholders to implement sustainable energy consumption.

The study of Erdogan et al., [19], found that the policies and practices of hotels generally lack attributes relevant to environmental protection and conservation. Hotel managers mostly lack the necessary environmental knowledge and interest to meet the basic objectives of social and environmental responsibility. They propose the development of an integrated system of policy and practice that involves not only the hotel management and staff, but also all parties concerned with environmental protection and sustainability. Further, they suggest the re-evaluation and reconsidering of the national, local, and hotel policies and training activities. Hirschl et al., [20], argued that the decisive factor in the successful implementation of sustainable use patterns occurs as shift of use regimes. Strategic players are, according to Hirschl et al., [20], ‘change agents’ that enable the change of sustainable effectiveness of the hotel organizational culture. There are many positive examples of how to shift cognitions toward development of a sustainable organizational culture in hotels. Karagiorgas et al., [22],

applied the basic model of the energy flow through the hotel interface from fuel input through eight cost centres and down to five end-use services using an energy mix matrix. Their results show that energy consumption considerably varies, and that their model can be used to analyse higher energy consumption areas. Trung and Kumar, [23], reported the results of a study conducted to assess the resource use and management in the hotel industry in Vietnam. The current practices in the hotels address energy and water consumption, and waste generation. These issues are highlighted, and benchmarks for the efficient use of resources in Vietnamese hotels are presented. Bohdanowicz and Zientara' s [24] study showed that hotels can be very wasteful and consume huge amounts of resources. It has been estimated that seventy-five percent of hotels' environmental impacts can be directly related to excessive consumption.

There is a strong need to change the consumption behaviour. This can be achieved by making hotels green. Departmental audits are essential to determining where the efforts should be focused. All operations generating GHG can be incorporated as indicators in such audits. Without the support of employees, an environmental program is doomed to fail. Employees are in the core of operations and are familiar with the behaviour of all stakeholders toward the consumption of resources.

Our study aims at analysing the sustainable behaviour in hotels in Posavje, which is the result of their organizational culture. This argument led us to focus on the future expectations of the energy consumption, which are embedded in the organizational culture of the Posavje hotels. We sought to explore the mission dimension of the emerging green culture to discover the future changes in this field. There was one clear statement guiding the future behaviour regarding the sustainable behaviour and energy consumption:

/H1/: The mission dimension of the organizational culture of our hotel supports the changes toward the greening behaviour.

4 METHODOLOGY

To analyse the future orientation of the hotels toward the sustainable consumption of energy, we conducted quantitative analysis using nonparametric method Spearman Rank Order Correlations and descriptive statistics.

4.1 Participants

To measure the changes of organizational culture toward the sustainable consumption of the resources, we involved 47 employees from 13 hotels in Posavje. The sample included 23 men and 24 women. Ages of the participants ranged from 15 to 59.

***Table 1**: Sample features*

Feature	Frequency	Percentage
Education		
Preliminary school	1	2. 13
High school	22	46.81

College	23	48.94
Master	1	2.13
Sex		
Male	23	48.94
Female	24	51.06
Age		
15.625<x<=24.37	5	11
24.37<x<=33.125	19	40
33.125<x<=41.875	10	21
41.875<x<=50.625	11	23
50.625<x<=59.3750	2	4

4.2 Instrument

The survey instrument was custom-designed. The 11-item questionnaire tackled the long-term planning, the quality of culture change, the mission of the sustainable behaviour, and the employees' inclusion in the culture change in a hotel. We interspersed items from the scales randomly throughout the instrument. Each was accompanied by a five point-scale in a Likert format (1 = strongly agree, 5 = strongly disagree) for all items.

5 RESULTS

A univariate statistics procedure was used to analyse the survey data about the attitudes toward sustainable behaviour in the hotel. The green culture of the hotel is based on the concept of sustainable tourism. It is the realization of the successful behaviour of all employees and other stakeholders regarding energy consumption. Results show that employees in the hotels included in our study somehow build the new energy consumption behaviour, which is manifested through the proposed 'green' behaviour:

- Energy consumption strategy,
- Innovative governance of waste and waste water,
- Waste water renewal,
- Protecting from fire, accidents and injuries,
- Changing of the solid waste to new energy,

- The use of new technologies for the energy preservation,
- Integrating of infrastructure systems on the level of hotel resorts and on the level of local community.

Respondents in the hotels Termana, Park Laško, Radenci, and City show positive attitudes toward the building of green culture. Some other hotels are at the beginning the process.

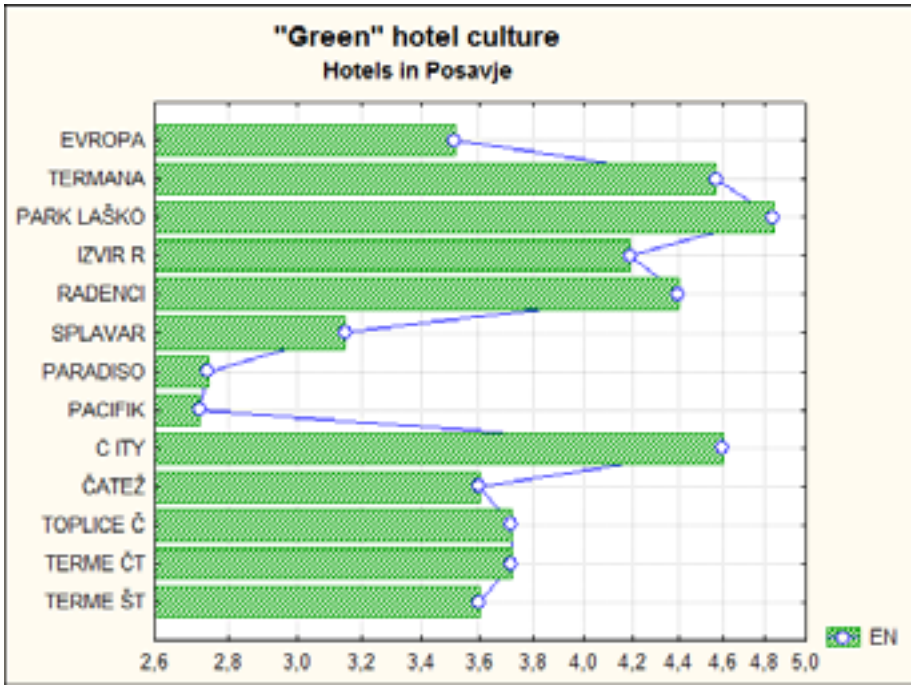

Figure 1: *The strength of an energy consuming behaviour*

The impact of organizational behaviour on the development of the green culture was manifest through the long-term vision of energy consumption, through the levelling of short and long-term goals, through the effort to find consensus about the energy consumption, and through the involvement of the employees in the change process. These attitudes are significantly correlated to the elements to the elements of the green culture of the hotels in the study.

Table 2*: Attitudes of respondents toward the green culture*

Attitudes of the respondents	Green culture	Mean	Std
The management of a hotel has a long-term vision of energy consumption.	0.32*	4.02	0.90
We are capable of realizing of the short-term goals	0.31*	4.02	0.74

without endangering the long-term goals.			
The consequences of our decision are often neglected interests of consumers and service buyers.	0.21	2.53	1.35
The mistakes we made in our business are always opportunities to learn.	0.27	4.13	0.74
We miss many opportunities regarding the new ways of energy consumption.	0.01	2.72	1.06
Our strategic decisions in the field of energy consumption are not clear.	-0.12	2.94	1.29
There is no 'special culture' in our hotel that impacts its sustainable development.	-0.12	2.94	1.21
We often have trouble finding the consensus about the sustainable energy and resources consumption in our hotel.	-0.32*	2.77	1.05
The collaboration with employees regarding the sustainable use of energy and resources is as difficult as the collaboration with competitive hotels.	-0.00	3.13	1.13
It is common in our hotel that we sacrifice our long-term goals for the realization of short-term goals.	-0.16	3.06	1.09
Employees and groups are involved in the process of implementing the sustainable changes.	0.45*	3.72	0.85
When the problems in energy consumption emerge, we always try to find a solution that suits everybody.	0.08	4.06	0.89

MD pairwise deleted Marked correlations are significant at p <.05000

The results show that behaviour oriented toward the building of a green culture lack the systematic orientation and collaboration of all stakeholders. Furthermore, there is no clear decision-making process about the energy consumption. Green culture is still weak and in the initial phases of development.

Building a green culture is an important competitive factor for the hotel business in the future. At the same time, it is a source of new innovative 'green' products that will inevitably replace classic tourism products that produce too many emissions. Much effort will be put into the change of behaviour toward more sustainable way of living and of doing business. Organizational culture functions as an identity of an organization. Its generation is embedded in the collective memory of organization. It is important to know that organizational culture can be changed when new and successful behaviours emerge and stabilize. When organizations are

---

innovative enough and when they have a support of the state and local community, a new green culture can emerge and give the tourism a new surge of creativity.

References

[1] **Denison, D. R.; Mishra, A. K.:** *Toward a Theory of Organizational Culture and Effectiveness*. Organization Science, 1995, Vol.6 No 2, pp. 204–222.

[2] **Che Jamil, M. F., Yusof, N., Said, I., Osman, Z.**: *Organizational Culture and performance of Resort Operators of a Lake-Based Tourism Area in Malaysia*. World Applied Sciences Journal, 2010, Vol. 10, No. 5: pp. 597–606.

[3] **Ambrož, M., Praprotnik, M.**: *Organisational effectiveness and customer satisfaction*. Organizacija (Kranj), 2008, Vol. 41, No. 5, pp. 161–173.

[4] **Gillespie, M. A., Denison, D. R., Haaland, S., Smerek, R., Neale, W. S.**: Linking *organizational culture and customer satisfaction: Results from tow companies in different industries.* European Journal of Work and Organizational Psychology, 2008, Vol 17, No 1, pp. 4–22.

[5] **Dhewato, W., Vitale, M., Sohal, A.**: *The effect of organizational culture on technology commercialisation performance: conceptual framework*, 2009, AGSE.

[6] **Denison, D. R.**: *Bringing corporate culture to the bottom line*, 1984, Organizational dynamics, Vol. 13, No 2, pp- 5–21

[7] **Denison, D. R.**: *Corporate culture and organizational effectiveness*, 1990, New York, Wiley.

[8] **Kelly, J.; Williams, P. W.**: *Modelling Tourism Destination Energy Consumption and Greenhouse Gas Emissions*: Whistler, British Columbia, Canada, 2007, Journal of sustainable tourism, Vol. 15, No. 1.pp. 67–90.

[9] **Bohdanowicz, P., Churie-Kallauge, A., Martinac, I.**: *Energy-Efficiency and Conservation in Hotels – Towards Sustainable Tourism*. 4th international Symposium on Asia Pacific Architecture, Hawai'i, April 2001

[10] **Ayuso, S.**: *Adoption of voluntary environmental tools for sustainable tourism: analysing the experience of Spanish hotels*. 2006, Corporate Social Responsibility and Environmental Management, Vol. 13, No.4, pp. 207–220.

[11] **Becken, S. and Simmons, D. G.**: *Understanding energy consumption patterns of tourist attractions and activities in New Zealand*, 2002, Tourism Management, Vol. 23, No.4, pp. 343–354.

[12] **Becken, S., Simmons, D. G., et al.**: *Energy use associated with different travel choices.* Tourism Management, 2003, Vol. 24, No. 3, pp. 267–277.

[13] **Becalli, M., La Gennusa, M. et al.**: *An empirical approach for ranking environmental and energy saving measures in the hotel sector*, 2009, Renewable Energy Vol. 34, No. 1, pp. 82–90.

[14] **Budeanu, A.**: *Sustainable tourist behaviour – a discussion of opportunities for change*, International Journal of Consumer Studies, 2007, Vol. 3, No.5, pp. 499–508.

---

[15] **Chan, W. W. and Lam, J. C.**: *Prediction of pollutant emission through electricity consumption by the hotel industry in Hong Kong*, 2002, International Journal of Hospitality Management, Vol. 21, No. 4, pp. 381–391.

[16] **Dalton, G. J., Lockington, D. A., et al.** (2008). *Feasibility analysis of stand-alone renewable energy supply options for a large hotel*, Renewable Energy, 2008, Vol. 33, No. 7, pp. 1475–1490.

[17] **Cole, M.**: *Cultural Psychology*. Cambridge, MA: Harvard University Press, 1996.

[18] **Schein, E.**: *Organizational culture and leadership*. San Francisco: Jossey-Bass., 1985.

[19] **Erdogan, N. and E. Baris, E.**: *Environmental protection programs and conservation practices of hotels in Ankara*, Turkey. Tourism Management, 2007, Vol. 28, No.2, pp. 604–614.

[20] **Hirschl, B., W. K., et al.**: *New concepts in product use for sustainable consumption*, 2003, Journal of Cleaner Production, Vol. 11, No. 8, pp. 873–881.

[21] **Karagiorgas, M. T. T., et al.**: *HOTRES: renewable energies in the hotels. An extensive technical tool for the hotel industry*, 2006, Renewable and Sustainable Energy Reviews 10(3): 198–224.

[22] **Karagiorgas, M., Tsoutsos, T. et al.**: *A simulation of the energy consumption monitoring in Mediterranean hotels: Application in Greece*, 2007, Energy and Buildings, Vol. 39, No. 7, pp. 416–426.

[23] **Trung, D. N., and S. Kumar**: Resource and waste management in Vietnam hotel industry, 2005, Journal of Cleaner production , Vol. 13, No., pp. 109-116.

[24] **Bohdanowicz, P. and Zientara, P.**: Corporate Social Responsibility in Hospitality: Issues and Implications. A Case Study of Scandic, 2008, Scandinavian Journal of Hospitality and Tourism, Vol. 8, No. 4, pp. 271-293.

JET Volume 5 (2012), p.p. 37 - 54

Issue 1, February 2012

http://www.fe.uni-mb.si/si/jet.html

SYSTEM CONTROL IN CONDITIONS OF DISCRETE STOCHASTIC INPUT PROCESS

UPRAVLJANJE SISTEMA V POGOJIH DISKRETNEGA SLUČAJNOSTNEGA VHODNEGA PROCESA

Janez Usenik[ℜ], Maja Repnik[1]

Keywords: power supply system, control, discrete random process, z-transform.

Abstract

In this article, a mathematical model of control for a discrete stochastic system, which can also be power supply system, is presented. Analytical approaches that can be used to describe the mutual impact of output and stocks (additional capacities) on hierarchically distributed occurrence/usage/variation or demand already exist. We add dynamics to the system. For this, we use discrete time functions, i.e. dynamic processes, which are of a random (stochastic) form, since our goal is to describe actual, concrete system as accurately as possible. We build a dynamic discrete model of control for this system with a system of difference equations, which can be solved with a one-part z-transform. Due to the stochastic inputs of the system, we can use a Wiener filter for discrete random processes to meet the requirement of optimality. With a z-transform, we convert the system of difference equations in a real time zone into system of algebraic equations in a complex area. First, we derive the Wiener-Hopf equation in a complex area; then we use spectral factorisation to obtain its solution, which has to be transformed back to real time zone with inverse z-transform. This is how we find the optimal solution of a given control problem. At the end of the article, we also demonstrate a numerical example with concrete form of input discrete random process.

[ℜ]Corresponding author: Prof. Janez Usenik, PhD., University of Maribor, Faculty of Energy Technology, Tel.: +386 40 647 689, Fax: +386 7 620 2222, Mailing address: Hočevarjev trg 1, SI-8270 Krško, Slovenia, e-mail address: janez.usenik@uni-mb.si

[1]University of Maribor, Faculty of Energy Technology, Krško

---

Povzetek

V članku je predstavljen matematični model upravljanja diskretnega stohastičnega (slučajnostnega) sistema. Ta sistem je lahko tudi energetski sistem. Razviti so analitični pristopi, s katerimi opišemo medsebojni vpliv proizvodnje ter zalog (dodatnih kapacitet) na hierarhično porazdeljeno prostorsko dogajanje/porabo/spremembo oziroma povpraševanje. V sistem vpeljemo dinamiko, kar storimo z uporabo diskretnih časovnih funkcij – dinamičnih procesov, ki pa so zaradi zahteve po čim tesnejšem približku opisovanja dejanskega sistema, slučajnostne (stohastične) narave. Dinamični diskretni model upravljanja takšnega sistema izgradimo s sistemom diferenčnih enačb, ki ga rešimo z uporabo enostrane z-transformacije. Pogoju optimalnosti lahko zaradistohastičnih vhodov sistema zadostimo z uporabo Wienerjevega filtra za diskretne slučajnostne procese. Z uporabo z-transformacije pretvorimo sistem diferenčnih enačb v realnem časovnem prostoru v sistem algebrajskih enačb v kompleksni ravnini. Na ta način najprej izpeljemo Wiener-Hopfovo enačbo v kompleksni ravnini, njeno rešitev pa dobimo v nadaljevanju z metodo spektralne faktorizacije. Z uporabo inverzne z-transformacije izračunamo optimalno rešitev danega problema upravljanja v realnem časovnem prostoru. Ob koncu članka je prikazan šenumerični primer, v katerem vzamemo konkretno obliko vhodnega diskretnega slučajnostnega procesa.

1 INTRODUCTION

Every real system (power supply, logistics, traffic, etc.) is a very complex dynamic system. In creating their theoretical mathematical model, we would have to take into account an extremely large number of variables and their interrelationships. However, with methods of logical and methodological decomposition, a system may be divided into a finite set of simpler subsystems, which are then studied and analysed separately, [1].

A model of optimal control is determined with a system, input variables and the optimality criterion function. The system represents a regulation circle, which generally consists of a regulator, a control process, a feed-back loop, and input and output information. In this article, we will only discuss linear dynamic stationary discrete systems. The optimality criterion is the standard against which the control quality is evaluated. The term 'control quality' means optimal and synchronized balancing of planned and actual output functions, [2, 3].

Let us consider a production model in a linear stationary dynamic system in which the input variables indicate the demand for products manufactured by a company. These variables, i.e. the demand in this case, can either be a one-dimensional or multi-dimensional vector functions or they can be deterministic, stochastic or fuzzy. In this article, stochastic variables are presented.

2 DEFINING THE PROBLEM

Beginning with a stationary random process, X, with the known mathematical expectation, $E(X)$, autocorrelation $R_{xx}(k)$ as the demand in a stochastic situation that should be met, if possible, by the current production. The difference between the current production and demand is the input function for the control process; the output function is the current stock/additional capacities. When the difference is positive, the surplus will be stocked, and when it is negative, the demand will also be covered from stock. Of course, in the case of a power supply, stock in the usual sense does not exist (such as cars or computers, etc.); energy

cannot be produced in advance for a known customer, nor can stock be built up for unknown customers. The demand of energy services is neither uniform in time nor known in advance. It varies, has its ups (maxima) and downs (minima), and it can only be met by installing and activating additional proper technological capacities. Because of this, the function of stock in the energy supply process is held by all the additional technological potential/capacities, large enough to meet periods of extra demand. The demand for energy services is not given and precisely known in advance. With market research, we can only learn about the probability of our specific expectations of intensity of demand. Demand is not given with explicitly expressed mathematical functions; we only know the shape and type of the family of functions. Demand is, accordingly, a random process for which all the statistical indicators are known.

The system input represents the demand for the products/services that a given subject offers. Let demand be a stationary random process with two known statistical characteristics: mathematical expectation and autocorrelation function, [4, 5]. Any given demand should be met with current production. The difference between the current capacity of production/services and demand is the input function for the object of control. The output function measures the amount of unsatisfied costumers or unsatisfied demand in general. When this difference is positive, i.e. when the power supply capacity exceeds the demand, a surplus of energy will be made. When the difference is negative, i.e. when the demand surpasses the capacities, extra capacities will have to be added or, if they are not sufficient, extra external purchasing will have to be done. Otherwise, there will be delays, queues etc. In the new cycle, there will be a system regulator, which will contain all the necessary data about the true state and that will, according to given demand, provide basic information for the production process. In this way, the regulation circuit is closed. With optimal control, we will understand the situation in which all costumers are satisfied with the minimum involvement of additional facilities. On the basis of the described regulation circuit, we can establish a mathematical model of power supply control, i.e. a system of difference equations for discrete systems, [6], in our situation. A mathematical model of control for this system will be structured around the theoretical model of control of linear stationary systems. For this model, the regulation circuit is given in Figure 1, [7].

The task is to determine the optimum production and stock/capacities, so that the total cost will be as low as possible.

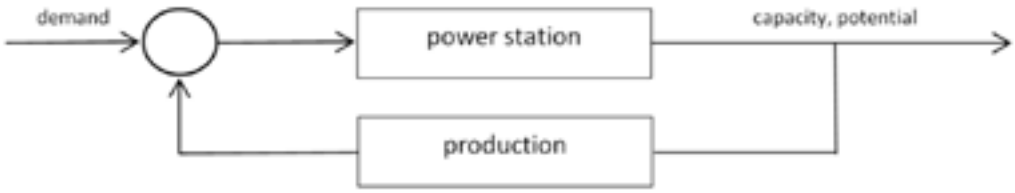

Figure1: *Regulation circuit of the power supply system*

---

3 A THEORETICAL MODEL OF THE SYSTEM CONTROL

In building of the model, we will restrict ourselves to dynamic linear system, in which the input is a random process with known statistical properties. The system provides the output which is, due to the condition of linearity, also a random process. These processes could be continuous or discrete. Model and its solving for continuous processes is obtained in [2]. So we will set up the mathematical model for discrete stochastic processes.

The optimization model of dynamic system regulation is determined by the system and by the optimality criterion. The system as regulation circuit generally consists of a regulator, the object of regulation, feedback, input and output information, [8], (See Figure 2).

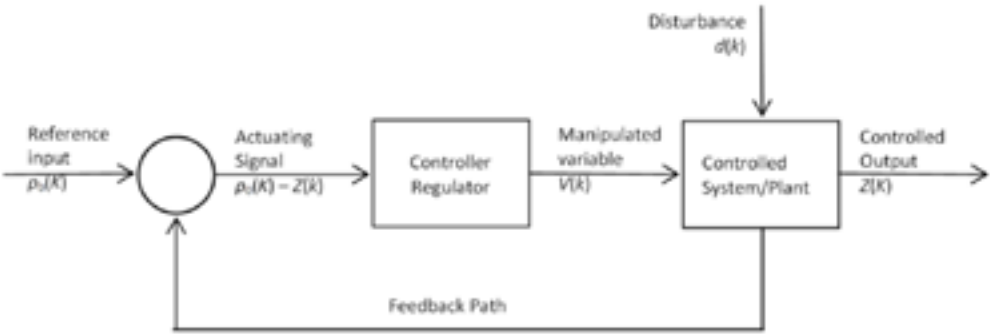

***Figure 2**: A regulation circuit*

From this point onward, let all functions be functions of discrete variable: $p_0 = p_0(k)$, $v = v(k)$, $Z = Z(k)$, $d = d(k)$, $k \in \mathbf{Z}$ and attention will solely be given to a linear stationary system. Considering this, the equations of the object of regulation and regulator are:

$$Z(k) = \sum_{\kappa=0}^{\infty} G_P(k-\kappa)\left[v(\kappa) - d(\kappa)\right]$$

$$v(k) = \sum_{\kappa=0}^{\infty} G_R(k-\kappa)\left[p_0(\kappa) - Z(\kappa)\right]$$

where $G_P(k)$ and $G_R(k)$ are operators of the object of regulation and regulator, respectively. If we use one-side z-transform and write these two equations in complex area, we obtain:

$$Z(z) = G_P(z)\left[v(z) - d(z)\right]$$

$$v(z) = G_R(z)\left[p_0(z) - Z(z)\right]$$

Here $G_P(z)$ and $G_R(z)$ denote transfer functions of object of regulation and regulator. Now let us presume that the transfer function of regulator is a product of two transfer functions:

$$G_R(z) = \tilde{G}_f(z) G(z).$$

Here $\tilde{G}_f(z)$ is a known function and $G(z)$ is unknown function, which can vary. $G(z)$ is called the operator of regulation.

In a concrete system control, like a power supply system, this kind of supposition is realistic and can depict real problems well.

Figure 3 depicts a block diagram of this kind of system. Here we added another operator: $s_i(z) = G_i(z)p_0(z)$. With this operator, we define ideal output variables.

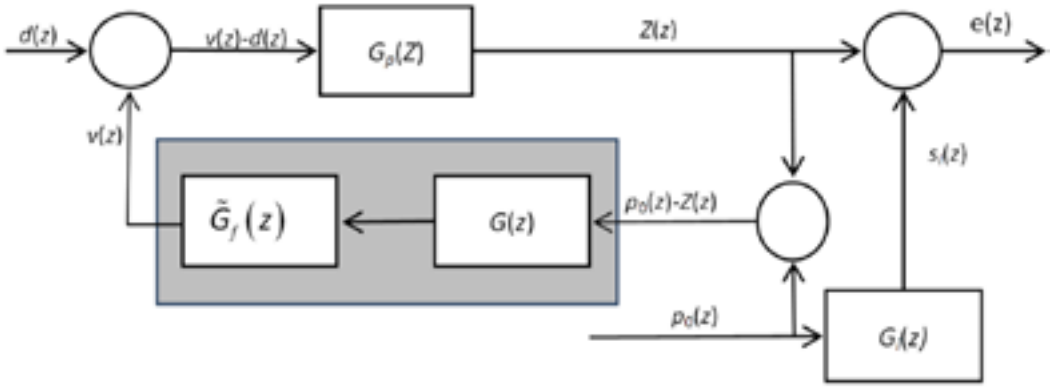

Figure 3: *Block diagram of discrete system control*

As in continuous systems, we will also use Wiener filter in the criterion function here. We are searching for minimum of the mean of square error $e(z)$.

This can be achieved if we determine the operator of regulation $G(z)$ as optimally as possible.

We can always obtain (with parallel shift) that the planned variable is equal to zero: $p_0(z) \equiv 0$, so the error (which we want to be as small as possible) is simply the output function of the system (Figure 4): $e(z) = s_i(z) - Z(z) = G_i(z)p_0(z) - Z(z) = -Z(z)$

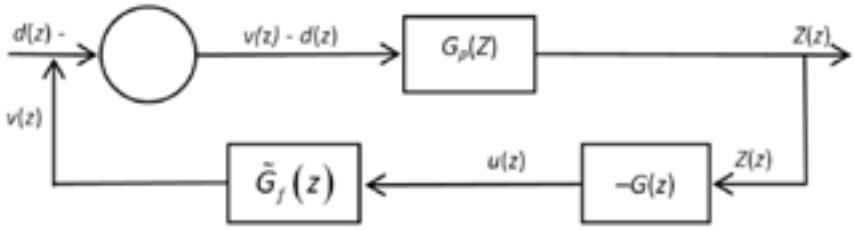

Figure 4: *Block diagram of discrete system control with factored operator of the regulation with* $p_0(z) \equiv 0$

It can be seen from the figure 4 that equations of the system are now:

$$Z(z) = G_P(z)\left[v(z) - d(z)\right] \tag{3.1}$$

$$v(z) = \tilde{G}_f(z)\,u(z) \tag{3.2}$$

$$u(z) = -G(z)Z(z) \tag{3.3}$$

(3.1) is equation of object of regulation, (3.2) and (3.3) are equations of regulator. $G_P(z)$ and $\tilde{G}_f(z)$ are known operators in concrete cases , while $G(z)$, which is the operator of regulation, should be determined in a such way that it will meet the requirements of the criterion function.

In discrete systems, the block diagram can be transferred into cascade form. This can make calculation of $G(z)$ much easier. As a solution of the Wiener-Hopf equation, we first obtain optimal cascade operator $W_{\text{opt}}(z)$ and after that the operator of regulation $G(z)$, that we searched for.

3.1 Wiener-Hopf equation for discrete system

Let the system in the real time zone be formed with these three discreet equations:

$$Z(k) = \sum_{\kappa=0}^{\infty} G_P(\kappa)\left[v(k-\kappa) - d(k-\kappa)\right] \tag{3.4}$$

$$v(k) = \sum_{\kappa=0}^{\infty} \tilde{G}_f(\kappa)\,u(k-\kappa) \tag{3.5}$$

$$u(k) = -\sum_{\kappa=0}^{\infty} G(\kappa)Z(k-\kappa) \tag{3.6}$$

Let $\{Z(k)\}$, $\{v(k)\}$, $\{u(k)\}$ and $\{d(k)\}$ denote stationary discreet random processes for all $k \in \mathbf{Z}$ in equations (3.4) to (3.6). Let the autocorrelation of input process $\{d(k)\}$ be known. For the criterion of optimality we shall use Wiener filter, so we have to determine the minimum of the mean of square error.

$$Q = K_Z E\left[\left(Z(k) - Z_0(k)\right)^2\right] + K_u E\left[\left(u(k) - u_0(k)\right)^2\right]$$

This equation now represents optimality criterion, where K_z and K_u denote two positive constants (weights) and expressions $\left[Z(k) - Z_0(k)\right]$ and $\left[u(k) - u_0(k)\right]$ represent the difference between actual functions and ideal functions, $Z_0(k)$ and $u_0(k)$, that are defined in advance for all $k \in \mathbf{Z}$. If $Z_0(k) \equiv 0$ and $p_0(k) \equiv 0$, (permissible because of parallel shift) the optimality criterion function in a simpler form is obtained:

$$Q = K_Z E\left(Z^2(k)\right) + K_u E\left(u^2(k-1)\right) \tag{3.7}$$

If we divide equation (3.7) with $K_z \neq 0$ and denote $P = \frac{Q}{K_z}$ and $A^2 = \frac{K_u}{K_z}$, we can write the criterion function in more useful form, which is:

$$P = E\left\{Z^2(k)\right\} + A^2 E\left\{u^2(k-1)\right\} \tag{3.8}$$

Now let us perform a z-transformation on all three equations of our mathematical model. Without loss of generality, it can be assumed that all initial conditions are equal to zero. We then obtain the equations:

$$Z(z) = G_P(z)\left[v(z) - d(z)\right] = G_P(z)v(z) - G_P(z)d(z)$$

$$v(z) = \tilde{G}_f(z)u(z)$$

$$u(z) = -G(z)Z(z)$$

If we denote $D(z) = G_P(z)d(z)$ and $G_f(z) = \tilde{G}_f(z)G_P(z)$ we can easily calculate

$$Z(z) = \frac{1}{-1 - G(z)G_f(z)} \cdot D(z)$$

Now we can write $u(z) = -G(z)Z(z) = W(z) \cdot D(z)$

where

$$W(z) = \frac{G(z)}{1 + G(z)G_f(z)} \tag{3.9}$$

So we can write:

$$u(z) = W(z)D(z)$$

$$Z(z) = \left[W(z)G_f(z) - 1\right]D(z) \tag{3.10}$$

$$V(z) = G_f(z)u(z)$$

With all of these denotations, we can draw a block diagram in cascade form (Figure 5):

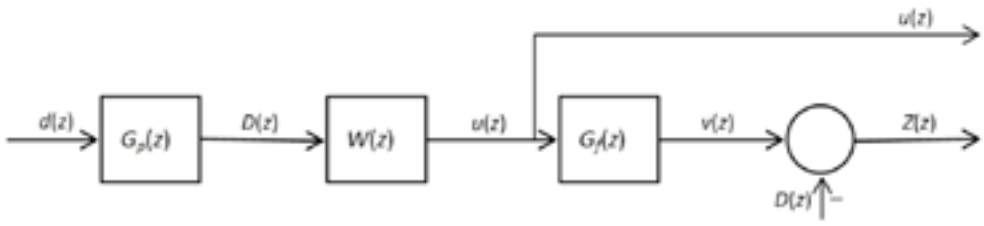

Figure 5: *Cascade operator of compensation*

If we denote $E\left(Z^2(k)\right)=R_{ZZ}(0)$ and $E\left(u^2(k)\right)=R_{uu}(0)$, we can also write the optimality criterion function in the form $Q=K_z R_{ZZ}(0)+K_u R_{uu}(0)$ or:

$$P=R_{ZZ}(0)+A^2 R_{uu}(0) \tag{3.11}$$

To obtain a shorter and clearer form, take $S(z)=G_f(z)D(z)$ and write expression (3.10) as:

$$Z(z)=W(z)S(z)-D(z)$$

Spectral densities of autocorrelations $R_{ZZ}(k)$ and $R_{uu}(k)$ are:

$$\Phi_{ZZ}(z)=\mathcal{Z}\left\{R_{ZZ}(k)\right\}=W(z)W\left(z^{-1}\right)\Phi_{SS}(z)-W(z)\Phi_{SD}(z)-W\left(z^{-1}\right)\Phi_{SD}(z)+\Phi_{DD}(z)$$

$$\Phi_{uu}(z)=\mathcal{Z}\left\{R_{uu}(k)\right\}=W(z)W\left(z^{-1}\right)\Phi_{DD}(z)$$

Now, let us these two equations transform in the time zone and insert them in (3.11). Since $W(k)=0$ for $k<0$, we have

$$\begin{aligned}P&=R_{ZZ}(0)+A^2R_{uu}(0)=\\&=\sum_{k=0}^{\infty}W(k)\sum_{j=0}^{\infty}W(j)R_{SS}(k-j)-2\sum_{k=0}^{\infty}W(k)R_{SD}(k)+R_{DD}(0)+A^2\sum_{k=0}^{\infty}W(k)\sum_{j=0}^{\infty}W(j)R_{DD}(k-j)\end{aligned} \tag{3.12}$$

From (3.12), we can calculate the optimum, using a calculus of variations. First we suppose that solution $W_{\text{opt}}(t)$ exists and after that fix

$$W(t)=W_{\text{opt}}(t)+\eta W_{\eta}(t) \tag{3.13}$$

In (3.13), expression $W_{\eta}(t)$ is a possible weight, which represents the response of given system on input signals; therefore, it means a variation of function $W(t)$, η is calling variation parameter, which can be changed with regard to conditions, while $W_{\text{opt}}(t)$ is a solution of equation (3.12). Functions $W(t)$ and $W_{\eta}(t)$ have to meet the causality condition, meaning $W(k)=0$ for $k<0$.

If we write (3.13) in optimality criterion (3.12), then $P=P(\eta)$ and

$$\begin{aligned}P=&\sum_{k=0}^{\infty}W_{\text{opt}}(k)\sum_{j=0}^{\infty}W_{\text{opt}}(j)R_{SS}(k-j)-2\sum_{k=0}^{\infty}W_{\text{opt}}(k)R_{SD}(k)+R_{DD}(0)+A^2\sum_{k=0}^{\infty}W_{\text{opt}}(k)\sum_{j=0}^{\infty}W_{\text{opt}}(j)R_{DD}(k-j)+\\&+2\eta\left\{\sum_{k=0}^{\infty}W_{\eta}(k)\left[\sum_{j=0}^{\infty}W_{\text{opt}}(j)\left(R_{SS}(k-j)+A^2R_{DD}(k-j)\right)-R_{SD}(k)\right]\right\}+\\&+\eta^2\left[\sum_{k=0}^{\infty}W_{\eta}(k)\sum_{j=0}^{\infty}W_{\eta}(j)R_{SS}(k-j)+A^2\sum_{k=0}^{\infty}W_{\eta}(k)\sum_{j=0}^{\infty}W_{\eta}(j)R_{DD}(k-j)\right]\end{aligned}$$

The extreme of function $P(\eta)$ will exist, if expression at η would be equal to zero. For a minimum, the coefficient of the second variation must be positive. Thus, we have:

$$\sum_{k=0}^{\infty} W_{\eta}(k)\left[\sum_{j=0}^{\infty} W_{\text{opt}}(j)\left(R_{SS}(k-j)+A^2R_{DD}(k-j)\right)-R_{SD}(k)\right]=0 \tag{3.14}$$

Due to the causality condition, the expression in square brackets is equal to zero and (3.14) will always be true. This is the Wiener-Hopf equation for stationary discrete stochastic systems described with equations (3.4) to (3.6):

$$\sum_{j=0}^{\infty} W_{\text{opt}}(j)\left[R_{SS}(k-j)+A^2R_{DD}(k-j)\right]-R_{SD}(k)=0 \ , k \geq 0 \tag{3.15}$$

3.2 Solution of the Wiener-Hopf equation

Let us now initiate two additional discrete functions $\vartheta_1(i)$ and $\vartheta_2(i)$:

$$R_{SS}(k)+A^2R_{DD}(k)=\sum_{i=0}^{\infty}\vartheta_1(i)\,\vartheta_1(i+k) \tag{3.16}$$

$$R_{SD}(k)=\sum_{i=0}^{\infty}\vartheta_1(i)\,\vartheta_2(i+k) \tag{3.17}$$

with characteristic:

$$\vartheta_1(i)=0 \text{ for all } i<0 \tag{3.18}$$

With this substitution, we can simplify Wiener-Hopf equation (3.15):

$$\sum_{i=0}^{\infty}\vartheta_1(i)\left[\sum_{j=0}^{\infty} W_{\text{opt}}(j)\vartheta_1(i+k-j)-\vartheta_2(i+k)\right]=0\,,k\geq 0 \tag{3.19}$$

If we write *m* instead of *i+k* and take into consideration that (3.19) always holds, when the expression in square brackets is equal to zero, we obtain:

$$\sum_{j=0}^{\infty} W_{\text{opt}}(j)\vartheta_1(m-j)-\vartheta_2(m)=0\,,m>0 \tag{3.20}$$

With a one-sided z-transformation on equation (3.20), we get: $W_{\text{opt}}(z)\vartheta_1(z)-\vartheta_2(z)=0$ and from here solution of Wiener-Hopf equation in complex plane:

$$W_{\text{opt}}(z)=\frac{\vartheta_2(z)}{\vartheta_1(z)} \tag{3.21}$$

First, we need to compute both additional discrete functions $\vartheta_1(z)$ and $\vartheta_2(z)$ and then perform inverse z-transform. Let us first find function $\vartheta_1(z)$. From (3.18), it is obvious that its one-sided z-transform is the same as its two-sided z-transform:

$$\vartheta_1^{(2)}(z)=\vartheta_1(z) \tag{3.22}$$

From equation (3.16), we obtain the expression:

$$\vartheta_1(z)\,\vartheta_1\left(z^{-1}\right)=\Phi_{SS}(z)+A^2\Phi_{DD}(z)=\left[G_f(z)G_f\left(z^{-1}\right)+A^2\right]\Phi_{DD}(z) \tag{3.23}$$

In fact, this was spectral factorisation of the right side of equation (3.23). Because of its definition, discrete function $\vartheta_1(k)$ has its zeros and poles only in interior of unit circle. If zeros and poles are on the edge of the unit circle (on the curve), we perform the same action as with continuous systems. In this case, we can also multiply the left side of equation with $z^j z^{-j}=1$ and obtain:

$$\vartheta_1(z)\,\vartheta_1\left(z^{-1}\right)=z^j\vartheta_1(z)z^{-j}\vartheta_1\left(z^{-1}\right)=\left[z^j\vartheta_1(z)\right]\left[\left(z^{-1}\right)^j\vartheta_1\left(z^{-1}\right)\right],j\in\mathbf{Z}$$

For the additional discrete function $\vartheta_2(k)$ we did not make such demands as for $\vartheta_1(k)$; thus, if we perform two-sided z-transform on equation (3.17), we obtain:

$$\Phi_{SD}(z)=\vartheta_1\left(z^{-1}\right)\vartheta_2^{(2)}(z)$$

and

$$\vartheta_2^{(2)}(z)=\frac{\Phi_{SD}(z)}{\vartheta_1\left(z^{-1}\right)}$$

From the condition of minimum objective function optimal operator $W(z)$, i.e. the solution of Wiener-Hopf equation, the following is calculated, [1]:

$$W_{opt}(z)=\frac{\left[\dfrac{G_f\left(z^{-1}\right)\Phi_{DD}^{+}(z)}{\left(G_f(z)G_f\left(z^{-1}\right)+A^2\right)^{-}}\right]_{+}}{\left(G_f(z)G_f\left(z^{-1}\right)+A^2\right)^{+}\Phi_{DD}^{+}(z)} \tag{3.24}$$

where:

$$\Phi_{DD}(z)=\Phi_{DD}^{+}(z)\Phi_{DD}^{-}(z)\text{ and }A^2=K_u/K_z\,.$$

4 A DISCRETE STOCHASTIC MODEL OF THE ENERGY SYSTEM

Let us denote:

$Z(k)$ - activated facilities (resources) at given moment,

$u(k)$ - the amount of services performed (production) at given moment,

$d(k)$ - the demand for services at given moment,

$k\in\{0,1,2,\ldots\}$,

λ - time elapsed between the moment the data are received and the carrying out of a service,

Q - criterion function, complete costs,

K_z - constant coefficient, dependent from activated resources, derived empirically,

K_u - constant coefficient, dependent from performed services and derived empirically.

Assuming that the input variable demand is a stationary random process, we can also consider production and stock/additional capacities to be stationary random processes for reasons of the linearity of the system. Let us consider the functions $Z(k)$, $u(k)$ and $d(k)$ to be discrete stationary random processes.

The system will be modelled with the following equations:

$$Z(k)-Z(k-1)=\psi\left[v(k)-d(k)\right],\ \psi\in\mathbf{R}^{+} \tag{4.1}$$

$$v(k)=u(k-\lambda),\ \lambda\in N \tag{4.2}$$

$$u(k)=-\sum_{\kappa=0}^{\infty}G(\kappa)Z(k-\kappa) \tag{4.3}$$

$$Q(k)=K_z E\left\{\left(Z^2(k)\right)\right\}+K_u E\left\{\left(u^2(k-1)\right)\right\}\ minimum \tag{4.4}$$

In equation (4.3), the function $G(k)$ is the weight of the regulation that must be determined at optimum control, so that the criterion of minimum total cost is satisfied. The parameter λ, named 'lead time', is the time period needed to activate the additional capacities in the power supply process. We used a real situation in which any goods can be sold to the customer only from the 'storehouse of finished goods' because only in this case can the information flow of a company be updated and in accordance with legislation.

In (4.4), K_z and K_u are positive constant factors, attributing greater or smaller weight to individual costs. Both factors have been determined empirically for the product and are therefore in the separate plant, [8].

Equations (4.1) to (4.4) represent a linear model of control in which we have to determine the minimum of the mean square error, if by means of a parallel shift we cause the ideal quantity to equal zero.

$G(k)$ is the regulation function which, with optimum regulation, we want to define in such a way that the demand for minimum total costs will be met. We are looking for a system control with minimum operation costs $Q(k)$. The total costs (4.4), whose minimum we are looking for, is expressed with mathematical expectation (mean value) of the square of random variables $Z(k)$ and $u(k)$.

Equations (4.1) to (4.4) form a stationary stochastic linear model of control in which the minimum of criterial function is calculated on the basis of Wiener's filter. This means sought after solution using Wiener-Hopf´s equation will be obtained for these cases.

Indicating z-transforms: $Z\left\{Z(k)\right\}=Z(z)$, $Z\left\{v(k)\right\}=v(z)$, $Z\left\{d(k)\right\}=d(z)$, $Z\left\{u(k)\right\}=u(z)$ and applied to equations (4.1) to (4.3):

$$Z(z)=\frac{\psi z}{z-1}\left(v(z)-d(z)\right),\quad \psi\in \mathrm{R}^{+},$$

$$v(z)=z^{-\lambda}u(z)$$

$$u(z)=-G(z)Z(z)$$

Using the following notations:

$G_p(z)=\tilde{G}_f(z)G(z)$

$\tilde{G}_f(z)$ - fixed and initially defined operator,

$G(z)$ - unknown variable operator of regulation, compensation element,

$p_0(z)$ - desired (planned) output function,

$Z(z)$ - actual output function,

$s_i(z)=G_i(z)p_0(z)$ - ideal output,

$e(z)=s_i(z)-Z(z)$ - error, i. e. the difference between the ideal and actual output,

a regulation circle can now be drawn in the form of a block diagram (Figure 3). We are looking for the minimum of the mean square error $e(z)$.

Put more simply, the expressions are defined as follows:

$$D(z)=G_p(z)d(z)$$

$$G_f(z)=\tilde{G}_f(z)G_p(z)$$

$$V(z)=G_f(z)u(z)$$

$$P(z)=G_f(z)D(z)=G_f(z)G_p(z)d(z) \tag{4.5}$$

Using cascade compensation

$$W(z)=\frac{G(z)}{1+G(z)G_f(z)}$$

we may draw the flow chart in a simpler cascade form (Figure 5).

The searched-for optimum control operator $G(z)$ is obtained from optimal cascade compensation operator $W_{\text{opt}}(z)$ with the formula:

$$G_{\text{opt}}(z)=\frac{W_{\text{opt}}(z)}{1-W_{\text{opt}}(z)G_f(z)}$$

Cascade compensation operator $W_{\text{opt}}(z)$ is obtained as a solution to Wiener-Hopf equation for discrete functions and is calculated by (3.24).

Finally, the obtained functions are transformed into time zone with inverse z-transform.

The operator of the control process is $G_p(z)=\frac{\psi z}{z-1}$, fixed part of the regulator operator is $\tilde{G}_f(z)=z^{-\lambda}$ and

$$G_f(z)=\tilde{G}_f(z)G_p(z)=\frac{\psi z^{1-\lambda}}{z-1}. \tag{4.6}$$

5 AN EXAMPLE

Let the autocorrelation function of demand $R_{dd}(k)$ be known, for example:

$$R_{dd}(k)=\xi^2 a^{|k|},\ 0<a<1 \tag{5.1}$$

The spectral density is:

$$\Phi_{dd}(z)=\xi^2\left[\frac{z}{z-a}+\frac{z^{-1}}{z^{-1}-a}-1\right]=\frac{C^2}{(z-a)(z^{-1}-a)},\ C^2=\xi^2(1-a^2)$$

and from (4.5) we have

$$P(z)=\frac{\psi^2 z^{2-\lambda}}{(z-1)^2}d(z)$$

$$\Phi_{DD}(z)=G_P(z^{-1})G_P(z)\Phi_{dd}(z)=\frac{\psi^2 C^2}{(z-1)(z-a)(z^{-1}-1)(z^{-1}-a)}$$

$$\Phi_{PD}(z)=G_f(z^{-1})\Phi_{DD}(z)=\frac{\psi^3 C^2 z^{\lambda-1}}{(z-1)(z^{-1}-1)^2(z-a)(z^{-1}-a)}$$

$$\Phi_{PP}(z)=G_f(z^{-1})G_f(z)\Phi_{DD}(z)=\frac{\psi^4 C^2}{(z-1)^2(z^{-1}-1)^2(z-a)(z^{-1}-a)}$$

Because of (4.6), we have

$$\left[G_f(z)G_f(z^{-1})+\rho^2\right]\Phi_{DD}(z)=\frac{\psi^2\rho^2C^2(z-z_1)(z-z_2)}{z(z-1)^2(z^{-1}-1)^2(z-a)(z^{-1}-a)}$$

where

$$z_{1,2}=\frac{x-\sqrt{x^2-4}}{2}\ \text{and}\ x=\frac{\psi^2+2\rho^2}{\rho^2}=\frac{\psi^2}{2}+2>2.$$

Because $x>2$, then $\sqrt{x^2-4}>0$ and $z_1=\dfrac{x-\sqrt{x^2-4}}{2}<1$, $z_2=\dfrac{x+\sqrt{x^2-4}}{2}>1$.

From there

$$\left(G_f(z)G_f(z^{-1})+\rho^2\right)^{+}\Phi_{DD}^{+}(z)=\frac{\psi\rho C}{\sqrt{z_1}}\frac{(z-z_1)z^2}{(z-1)^2(z-a)}$$

Similarly, we can obtain

$$\left[\frac{G_f\left(z^{-1}\right)\Phi_{DD}^{+}(z)}{\left(G_f(z)G_f\left(z^{-1}\right)+\rho^2\right)^{-}}\right]_{+}=\frac{\psi^2C\sqrt{z_1}}{\rho(1-a)}\left[\frac{z}{(z-1)(1-z_1)}-\frac{za^{\lambda+1}}{(z-a)(1-az_1)}\right]$$

and from (3.9) :

$$W_{opt}(z)=\frac{\psi z_1}{\rho^2(1-a)}\left[\frac{(z-1)(z-a)}{(1-z_1)(z-z_1)z}-\frac{a^{\lambda+1}(z-1)^2}{(1-az_1)(z-z_1)z}\right]=\frac{z-1}{z(z-z_1)}\left[U_1(z-a)-U_2a^{\lambda+1}(z-1)\right]$$

where

$$U_1=\frac{\psi^2z_1}{\rho^2(1-a)(1-z_1)},\ U_2=\frac{\psi^2z_1}{\rho^2(1-a)(1-az_1)}$$

so that there are:

a) optimum production (the services) performed comply with function

$$u(z)=W_{opt}(z)G_P(z)d(z)=\left(U_1\frac{z-a}{z-z_1}-U_2\frac{a^{\lambda+1}(z-1)}{z-z_1}\right)d(z)$$

b) for $V_1=U_1-U_2a^{\lambda+1}$ and $V_2=U_1(z_1-a)-U_2a^{\lambda+1}(z_1-1)$ optimum stock (the facilities that were operating) involved comply with function:

$$Z(z)=G_f(z)u(z)-D(z)=\frac{\psi z^{1-\lambda}}{z-1}u(z)-D(z)=\left(\frac{V_1}{z^{\lambda}}+\frac{V_2}{z-z_1}-1\right)D(z)$$

With inverse z- transform, we obtain these functions in the time area:

a) optimum production:

$$\begin{aligned}u_{opt}(k)&=Z^{-1}\left\{u(z)\right\}=V_1d(k)+V_2\sum_{k'=1}^{\infty}z_1^{k'}d(k-k')=\\&=V_1d(k)+V_2\left[z_1d(k-1)+z_1^2d(k-2)+z_1^3d(k-3)+\cdots\right]\end{aligned}\qquad(5.2)$$

---

b) total optimal stock:

$$Z_{opt}(k)=\boldsymbol{Z}^{-1}\{Z(z)\}=V_1D(k-\lambda)+V_2\sum_{k'=1}^{\infty}z_1^{k'}D(k-\lambda-k')-D(k)= \\ =V_1D(k-\lambda)-D(k)-V_2\left[z_1D(k-\lambda-1)+z_1^2D(k-\lambda-2)+\cdots\right] \tag{5.3}$$

where $D(k)$ is total demand in a given time interval with changeable upper boundary:

$$D(k)=\boldsymbol{Z}^{-1}\{D(z)\}=\boldsymbol{Z}^{-1}\left(\frac{z}{z-1}\cdot d(z)\right)=\sum_{k'=0}^{k}d(k-k')=\psi\left(d(k)+d(k-1)+\cdots+d(1)+d(0)\right)$$

5.1 Discussion

In these data and results, parameters λ, a and A have influence on values of functions and so on the results of control. These parameters are involved in the constants V_1, V_2, U_1, U_2 and z_1.

I. According to constants V_1 and V_2 there are three possibilities:

1. $(V_1=0)\wedge(V_2=0)$

In this case, the system is degenerated completely. From (5.3) and (5.2) are $Z_{\text{opt}}(k)=-D(k)$ and $u_{\text{opt}}(k)\equiv 0$

The production of services equal zero that means the system does not work. The needs for capacities are only registered and equal the common demand in given time interval. The system of equations $(V_1=0)\wedge(V_2=0)$ is possible only for $a=1$, but in (5.1) we have condition $0<a<1$, which means that this situation is not possible.

2. $(V_1=0)\wedge(V_2\neq 0)$

In this case, there is a very unpleasant situation because the optimal solution is

$$u_{\text{opt}}(k)=V_2\sum_{\kappa=1}^{k}z_1^{\kappa}d(k-\kappa)$$

$$Z_{\text{opt}}(k)=V_2\sum_{\kappa=1}^{k}z_1^{\kappa}D(k-\lambda-\kappa)-D(k)$$

With which production is satisfied only the demand from the past and never from the present. It is the same with capacities. Such a situation is not optimal, because we would have permanent delays in working of the systems. From the equation $V_1=U_1-U_2a^{\lambda+1}=0$ we obtain

$$\lambda=\frac{\log\dfrac{1-az_1}{a(1-z_1)}}{\log a}$$

Because $0<a<1$, $\log\dfrac{1-az_1}{a(1-z_1)}>0$ and $\log a<0$, so $\lambda<0$. From the definition of delay, it is clear that $\lambda>0$. The condition $(V_1=0)\wedge(V_2\neq 0)$ is also impossible.

---

3. $(V_1 \neq 0) \wedge (V_2 = 0)$

In this case, the optimal solution is

$$u_{\text{opt}}(k) = V_1 d(k)$$

$$Z_{\text{opt}}(k) = V_1 D(k-\lambda) - D(k)$$

The production of services satisfies only present demand. It is possible to use the capacities with delay λ only for present demand. Furthermore, this control is not optimal, because it does not satisfy all needs of the system in throughout the duration of its working.

From $V_2 = U_1(z_1 - a) - U_2 a^{\lambda+1}(z_1 - 1) = 0$ we have

$$\lambda = \frac{\log \dfrac{(a - z_1)(1 - az_1)}{a(1 - z_1)^2}}{\log a}$$

Because of the value of the parameters a and z_1 we would obtain $\lambda < 0$. The condition $(V_1 \neq 0) \wedge (V_2 = 0)$ is also impossible.

The system will be controlled optimal when the constants V_1 and V_2 are not equal zero. This condition is true for $0 < a < 1$.

II. According to parameters K_u and K_z there are two possibilities:

a) $K_u > K_z$,

b) $K_u < K_z$.

The expression

$$\sum_{\kappa=1}^{\infty} z_1^{\kappa} d(k-\kappa) = z_1 d(k-1) + z_1^2 d(k-2) + z_1^3 d(k-3) + z_1^4 d(k-4) + \cdots$$

is convergent faster for $K_u > K_z$ than for $K_u < K_z$. That means the production of services depends on the demand in a given moment more than from previous demand. For that reason we will cover the demand with extra capacities.

In the second case ($K_z > K_u$), the storing and activating of extra capacities is very expensive and we have to cover the demand with present capacities, i.e. the present production of services.

6 CONCLUSION

A theoretical mathematical model of system control can also be used in an energy technology system and in all their subsystems. Input-output signals are whether discrete or continuous functions. For operations, many conditions have to be fulfilled. During the control process, a great deal of information must be processed, which can only be done if a transparent and properly developed information system is available. During the operations, an enormous amount of data is used. The solutions, i.e. optimal control functions, depend on many numerical

parameters. All data and numerical analysis can only be processed into information for control if high quality and sophisticated software and powerful hardware are available.

For the study of structure, interrelationships and operation of a phenomenon with system characteristics, the best method is the general systems theory, and (within it) the systems regulation theory. When we refer to system technology as a synthesis of organization, information technology and operations, we have to consider its dynamic dimension when creating a mathematical model. As each such complex phenomenon makes up a system, the technology in this article is again dealt with as a dynamic system. Elements of the technological system compose an ordered entity of interrelationships and thus allow the system to perform production functions. Because of the condition of linearity, the response functions of the system are, with reference to the type of traffic, either continuous or discrete. During the control process, a great deal of information must be processed, which can only be done if a transparent and properly developed information system is available. During the operation of the power station, an enormous amount of data is used, which can only be processed into information for control if high quality software and powerful hardware are available. Communications also play a major role, as it is necessary to contact and use a number of international databases interactively. Models of optimum control can also be used in the power station system. The mathematical model with which we are describing the system can be analytically more or less complex, but generally the procedure always follows the same rule. With appropriate computer tools, an algorithm (which has not been presented in this article) can be used for concrete numerical examples.

References

[1] **J. Usenik, Ž. Radačić, S. Pavlin**: Airport system control in conditions of discrete random processes of traffic flow. *Promet-Traffic-Traffico* (Zagreb), 1998, 10, no. 1–2, pp. 1–4.

[2] **J. Usenik**: Mathematical model of the power supply system control. *Journal of Energy Technology*, Aug. 2009, vol. 2, iss. 3, str. 29-46.

[3] **J.J DiStefano, A.R. Stubberud, I.J.Williams**: *Theory and Problems of Feedback and Control Systems*, McGraw-Hill Book Company, 1987.

[4] **J. Usenik**: Control of Traffic System in Conditions of Random or Fuzzy Input Processes, *Promet-Traffic-Traffico*, 2001, Vol. 13 no. 1, pp. 1–8.

[5] **C. Schneeweiss**: *Regelungstechnische stochastische Optimierung Verfahren in Unternehmensforschung und Wirtschsaftstheorie*, Springer Verlag, Berlin, 1971.

[6] **J. Usenik:** Fuzzy dynamic linear programming in energy supply planning, *Journal of energy technology*, 2011, vol. 4, iss. 4, pp. 45-62.

[7] **J. Usenik, M. Bogataj**: A fuzzy set approach for a location-inventory model. *Transp. plann. technol.*, 2005, vol. 28, no. 6, pp. 447–464.

[8] **M. Bogataj, J. Usenik**: Fuzzy approach to the spatial games in the total market area. *Int. j. prod. econ*. [Print ed.], 2005, vol. 93–94, pp. 493–503.

JET Volume 5 (2012), p.p. 55 - 84

Issue 1, February 2012

http://www.fe.uni-mb.si/si/jet.html

COMPUTER SIMULATION OF A DIESEL SPRAY IGNITION AND COMMON RAIL ACCUMULATOR FUEL-INJECTION SYSTEM

RAČUNALNIŠKA SIMULACIJA SAMOVŽIGA DIZELSKEGA SPREJA IN VBRIZGALNEGA SISTEMA S SKUPNIM VODOM

Zdravko Praunseis[ℜ], Simon Marčič[1], Jurij Avsec[1], Milan Marčič[2]

Keywords: thermodynamics, combustion, diesel engine

Abstract

This paper describes a diesel fuel injection process and a diesel spray formation. A computer simulation of the common rail accumulator fuel-injection system and diesel spray were carried out. The computer simulation enables the observation of the phenomena from rail pressure, which is input data for the calculation of injection parameters, to self-ignition in the diesel combustion chamber. With computer simulation, the pressure values in specific sections of the injection nozzle may be computed, as well as the needle lift, injection rate and total injected fuel. The injection rate is input data for the simulation of the spray. The spray is divided into small elementary volumes in which the amount of fuel and fuel vapour, air, mean, maximum and minimum fuel droplet diameter as well as their number are calculated. In each elementary volume, the total air-fuel ratio and air-fuel vapour ratio are calculated. a new criterion for determining the self-ignition nuclei is described in the paper, based on assumptions that the strongest self-ignition probability lies in those elementary volumes containing the stoichiometric air ratio, where the fuel is evaporated or the fuel droplet diameter is equal to or

[ℜ] Corresponding author: Zdravko Praunseis, PhD, Faculty of Energy Technology, University of Maribor, Tel.: +386 31 743 753, Fax: +386 7 6202 222, Mailing address: Hočevarjev trg 1, Krško, Slovenia, E-mail address: zdravko.praunseis@uni-mb.si

[1] Faculty of Energy Technology, University of Maribor, Slovenia

[2]Faculty of Mechanical Engineering, University of Maribor, Slovenia

---

lower than 0.0065 mm. The most efficient combustion with regard to the consumption and emission will be in that elementary volume containing the stoichiometric air ratio and the fuel droplets with the lowest mean diameters. The injection and combustion parameter measurements were made in an optically accessible transparent engine. The engine is a single-cylinder transparent engine based on the AUDI V6 engine, equipped with a Bosch Common Rail Injection system. The optical part of the experimental set-up contains two different lasers, while the camera system allows the simultaneous detection of the Mie scattering of the injected fuel, the laser-induced fluorescence of fuel and vapour, the premixed combustion mode and the diffusion mode. A comparison of the computed points with the highest self-ignition probability and the measured points where self-ignition occurred showed good matching.

Povzetek

Članek opisuje proces vbrizgavanja dieselskega goriva in formiranja curka dieselskega goriva. V prikazanem članku je prikazan matematični model vbrizgalnega sistema. Curek goriva je v matematičnem modelu razdeljen na elementarne volumne, v katerih se izračunava količina goriva v plinasti in kapljeviti fazi, srednji, maksimalni in minimalni premer kapljic. V vsakem elementarnem volumnu se tudi izračunava razmerje zrak-gorivo v plinasti in kapljeviti fazi. V predstavljenem članku je prikazan nov kriterij za določitev samovžiga. Nov kriterij sloni na predpostavki, da največja verjetnost samovžiga leži v tistih elementarnih volumnih kjer je stehiometrični razmernik zrak-gorivo in kjer je premer kapljic manjši oz. enak kot 0.0065mm. Razen tega so v članku predstavljeni tudi eksperimentalni rezultati. Eksperimentalni rezultati so pridobljeni na študiji enovaljnega motorja, ki je osnovan na AUDI V6 motorju z Boschevim Common Rail vbrizgalnim sistemom in vgrajeno optično-lasersko merilno tehniko za določevanje lastnosti curka dieselskega goriva. Primerjava izračunanih in izmerjenih vrednosti za samovžig prikazuje dobro ujemanje rezultatov.

1 INTRODUCTION

Combustion is one of the most important contemporary sources of energy. Oil derivatives are currently the most frequently used fuels. Combustion-generated heat is utilised in process engineering, heating or converted by means of various machines into other forms of energy. Heat is most frequently converted into mechanical energy. Diesel engines convert the heat generated in hydrocarbon combustion into mechanical energy, most often used to power means of transport.

Due to their high thermal efficiency, diesel engines are primarily used in heavy- and medium-duty transport, while in recent decades they have also been increasingly used in passenger cars. This trend is particularly strong in Europe. Due to increasing requirements for lower fuel consumption and reduced pollution of the environment, designers are faced with increasingly challenging tasks. One of the most important processes influencing lower consumption and the reduced pollution of the environment by diesel engines is combustion. In contrast to Otto engines, where the ignition of the petrol vapour-air mixture is effected by a spark, in diesel engines the mixture is self-ignited. For efficient combustion, which is a pre-condition for low consumption and reduced pollution of the environment, it is very important to understand the nuclei, where self-ignition of the mixture occurs. Diesel engine loads vary during the operation and consequently also the position of the points in the combustion chamber, where nuclei for mixture self-ignition are formed.

One of the key elements affecting the combustion process is the fuel injection system, where the injection nozzle plays a decisive role in the dispersion of the fuel in the droplet-fuel vapour-air mixture in the combustion chamber. Therefore, we developed a computer simulation of the common rail accumulator fuel-injection system and diesel spray. Both computer programs enable computation of the injection and combustion parameters from the electric current at the triggering element (solenoid valve) to the self-ignition nuclei in the combustion chamber. Both programs are mutually connected. Spray calculation is impossible without knowledge of fuel injection process.

This paper describes a new self-ignition nuclei identification criterion to compute the probability that in a particular point of a diesel engine combustion chamber self-ignition occurs in the mixture between liquid fuel in droplets (fuel vapour-air). The computation of the probability of the mixture's self-ignition is based upon the following assumptions:

1. The highest efficiency of combustion in terms of fuel consumption and environmental pollution is at a stoichiometric air ratio.
2. Combustion efficiency and mixture self-ignition are influenced by the diameter of fuel droplets in the diesel spray. Fuel droplets with diameters of less than 0.0065 mm burn as if they were fuel vapours, which means that combustion will be the most complete if the entire fuel is evaporated or if droplets have diameters smaller than 0.0065 mm [1].

The highest probability of mixture self-ignition to occur is therefore at the stoichiometric air ratio points of the combustion chamber, and where practically most of the fuel is evaporated or the droplets have diameters of a few microns.

To compute the probability of mixture self-ignition, it is necessary to understand the fuel injection process and spray formation. Fuel injection in a transparent engine is carried out with a common rail injection system (Fig. 1). This paper describes a computer simulation of the common rail accumulator fuel-injection system. The input data for the injection parameter computation is the pressure in a high-pressure accumulator (rail) (Fig. 11) and the electric current at the triggering element (solenoid valve) (Fig. 10). By means of computer simulation, the pressure values in specific sections of the injection nozzle may be computed, as well as the needle lift, injection rate and total injected fuel. The injection rate is input data for simulation of the spray.

---

1 Air-mass meter, 2 ECU, 3 High-pressure pump, 4 High-pressure accumulator (rail), 5 Injectors, 6 Crankshaft-speed sensor, 7 Coolant-temperature sensor, 8 Fuel filter, 9 Accelerator-pedal sensor.

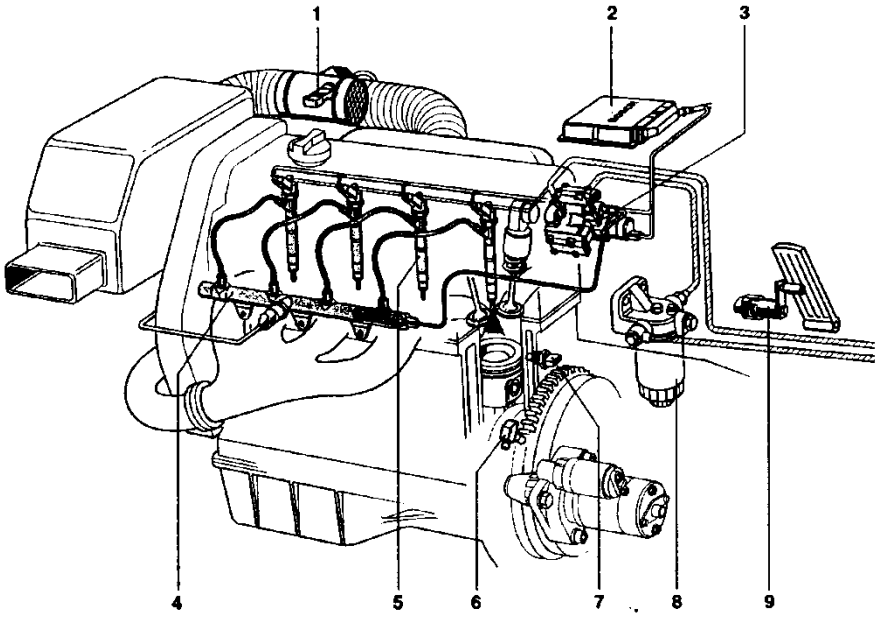

Figure 1: *Common Rail accumulator fuel-injection*

The spray is divided into small elementary volumes in which the amount of fuel and fuel vapours, air, mean, maximum and minimum fuel droplet diameter as well as their number is calculated. In each elementary volume, the total air-fuel ratio and air-fuel vapour ratio are calculated. Such data is used to compute the self-ignition probability in any elementary volume. Identical self-ignition probabilities are then joined into curves to obtain areas with equal self-ignition probabilities of the fuel vapour-air mixture.

The injection and combustion parameter measurements were made in an optically accessible, transparent engine. The engine is a single-cylinder transparent engine based on the AUDI V6 engine, equipped with a Bosch common rail injection system. The injection system can deliver pressures of up to 1350 bar. The optical part of the experimental set-up contains two different lasers, while the camera system allows the simultaneous detection of the Mie scattering of the injected fuel, the laser-induced fluorescence of fuel and vapour, the premixed combustion mode and the diffusion mode.

The comparison of the computed points with the highest self-ignition probability and the measured points where self-ignition occurred showed good matching.

2 MATHEMATICAL MODEL OF THE COMMON RAIL INJECTOR FUEL INJECTION SYSTEM

The highly efficient diesel engines for passenger cars are currently usually equipped with the common rail accumulator fuel-injection system (Fig. 1), which enables high pressure injection up to 2500 bars. High pressure injection means better spray formation and lower mean droplet

diameter. The Common Rail system is a modular system, and essentially the following components are responsible for these injection characteristics:

1. Solenoid-valve-controlled injectors, which are screwed into the cylinder head.
2. Pressure accumulator (rail).
3. High-pressure pump.

The following components are also required in order to operate the system:

1. Electronic control unit.
2. Crankshaft-speed sensor.
3. Camshaft-speed sensor.

This paper presents a mathematical model of a nozzle of solenoid-valve-controlled injector. Figure 2 shows the solenoid-valve-controlled injector and nozzle schematic. The input data for the injection parameter computation includes pressure at the inlet of the injector (Fig. 11) and the solenoid-valve pick-up current (Fig.10). They were both measured.

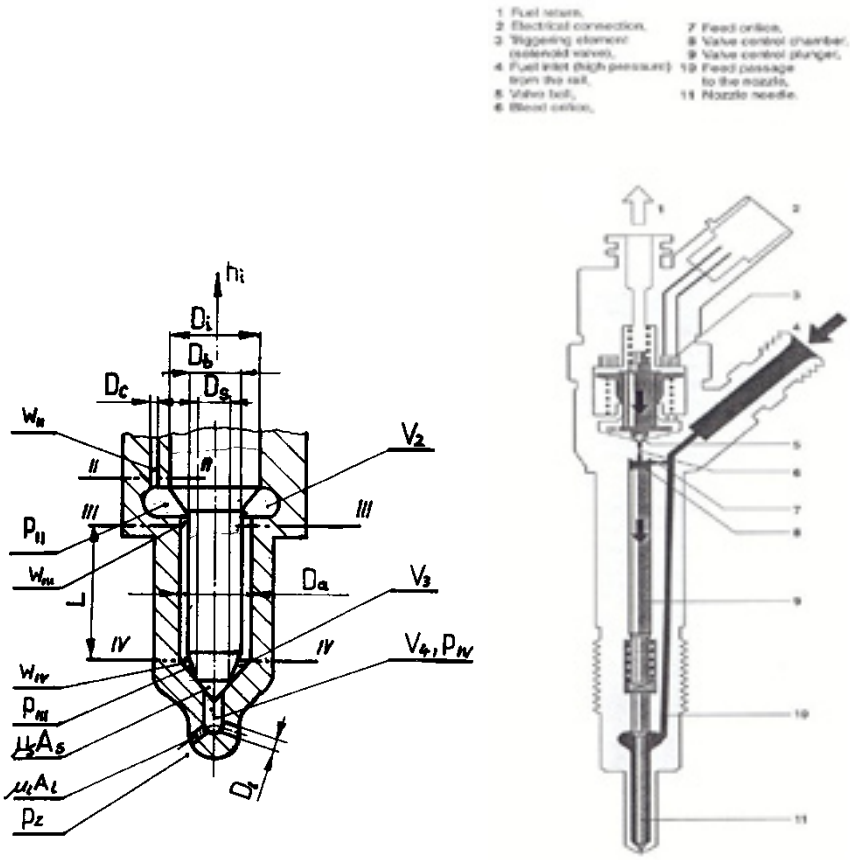

Figure 2: *Solenoid-valve-controlled injector and nozzle schema*

The assumption made in computation is that the pressure at the inlet of the injector (point 4, Fig. 2) and pressure, p_{II}, at the inlet of the nozzle are identical (cross section II-II, Fig. 2). The injection starts when the solenoid valve, 3, is energized with the pick-up current, which serves to ensure that injector opens quickly. The force exerted by the triggered solenoid, 3, now

---

exceeds that of the valve spring and the armature opens the bleed orifice. When the bleed orifice, 6, opens, fuel can flow from the valve-control chamber, 8, into the cavity situated above it, and from there via the fuel return, 1, to the fuel tank. This leads to the pressure in the valve-control chamber, 8, being lower than that in the nozzle's chamber volume V_2, which is still at the same pressure level as the rail. The reduced pressure in the valve-control chamber, 8, causes a reduction in the force exerted on the control plunger, 9, the nozzle needle opens as a result, and the injection starts. The force of the pressure on the needle of nozzle, 11, in the nozzle's chamber volume, V_2, has to overcome also the spring force, F_0, of the nozzle.

From pressure, p_{II}, we can calculate the velocity, w_{II}, of the fuel by equation (2.2, 2.3, 2.4)

$$w_{II} = \frac{1}{\rho a} p_{II} \tag{2.1}$$

The continuity equation for space V_2 is

$$w_{II} A_c - (A_i - A_b)\frac{dh_i}{dt} - w_{III}(A_a - A_b) - \frac{V_2}{E_{din}}\frac{dp_{II}}{dt} = 0 \tag{2.2}$$

For the calculation of pressure, p, and velocity, w, of fuel, we apply the Allevi theory [2]. It can be well supposed that the fluid flows only one way (in the direction of the pipe) because of the small diameter of the nozzle channel compared with its length. All frictional losses of fluid in the nozzle channel are neglected, because the nozzle channel is relatively short. The equations depicting the velocity and pressure in any point between cross sections III and IV are

$$\frac{\partial w}{\partial t} = -\frac{1}{\rho}\frac{\partial p}{\partial x}$$

$$\frac{\partial w}{\partial t} = -\frac{1}{\rho a}\frac{\partial p}{\partial t} \tag{2.3}$$

The two equations are solved by this particular solution:

$$p = p_0 + F(t - \frac{x}{a}) - W(t + \frac{x}{a}) + \ldots$$

$$w = \frac{1}{\rho a}\left[F\left(t - \frac{x}{a} \right) + W(t + \frac{x}{a}) + .. \right]. \tag{2.4}$$

With these general solutions, we can calculate the pressure and the velocity in any point between cross sections III and IV in the nozzle channel. The continuity equation of the volume V_3 is

$$w_{IV}\left(A_a - A_b\right) - \mu_s A_s\left(\sqrt{\frac{2}{\rho}}\right)\sqrt{p_{III} - p_{IV}} - A_b\frac{dh_i}{dt} - \frac{V_3}{E_{din}}\frac{dp_{III}}{dt} = 0. \tag{2.5}$$

The equation showing the dynamics of the needle, h_i (Fig. 3) is

$$m_i\frac{d^2h_i}{dt^2} + \left(d + d_1 + d_2\right)\frac{dh_i}{dt} + \left(k + k_1 - k_2\right)h_i + F_0 + F_{cr} - F_{tr} - p_{II}\left(A_i - A_b\right) - p_{III}\left(A_b - A_s\right) - p_{IV}A_s = 0, \tag{2.6}$$

where F_{tr} stands for friction and F_{cr} for solenoid force.

Boundary conditions for calculating the needle lift, h_i, are:

Time period I: Force on needle:

h_i=0

$$F_{cr} \neq 0, \quad p_{II}\left(A_i - A_b\right),$$

$$p_{III} = p_{IV} = 0,$$

$$k \neq 0, k_1 = 0, k_2 \neq 0$$

$$d \neq 0, d_1 = 0, d_2 \neq 0$$

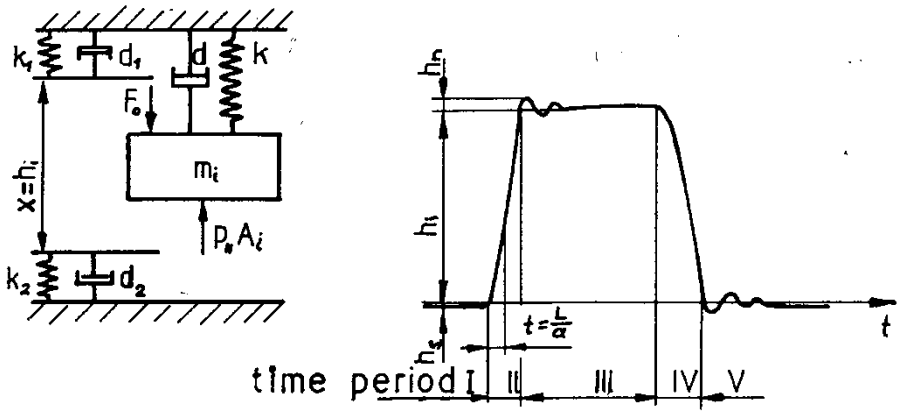

Figure 3: *Dynamics model of needle movement*

Time period II:

$$0 < h_i < h_{i\max} \qquad F_{cr} = 0, \quad p_{II}\left(A_i - A_b\right),$$

$$p_{III}\left(A_b - A_s\right),\ p_{IV}A_s$$
$$k \neq 0, d \neq 0$$
$$k_1 = k_2 = d_1 = d_2 = 0$$

Time period III:

$h_i=h_{imax}$ $$F_{cr} = 0,\ p_{II}\left(A_i - A_b\right),$$
$$p_{III}\left(A_b - A_s\right),\ p_{IV}A_s$$
$$k \neq 0, k_1 \neq 0, k_2 = 0$$
$$d \neq 0, d_1 \neq 0, d_2 = 0$$

Time period IV:

$0 < h_i < h_{i\max}$ $$F_{cr} \neq 0,\ p_{II}\left(A_i - A_b\right),$$
$$p_{III}\left(A_b - A_s\right),\ p_{IV}A_s,$$
$$k \neq 0, d \neq 0,$$
$$k_1 = k_2 = d_1 = d_2 = 0$$

Time period V:

$h_i = 0$ $$F_{cr} \neq 0,\ p_{II}\left(A_i - A_b\right),$$
$$p_{III}\left(A_b - A_s\right),\ p_{IV} = 0$$
$$k \neq 0, k_1 = 0, k_2 \neq 0$$
$$d = 0, d_1 = 0, d_2 \neq 0$$

Damping coefficients d, spring rates k and areas A are explained in Figure 3.

The continuity equation of the volume V_4 is

$$\mu_s A_s \sqrt{\frac{2}{\rho}} \sqrt{\left(p_{III} - p_{IV}\right)} - \mu_l A_l \sqrt{\frac{2}{\rho}} \sqrt{\left(p_{IV} - p_z\right)}.n - \frac{V_4}{E_{din}} \frac{dp_{IV}}{dt} = 0. \qquad (2.7)$$

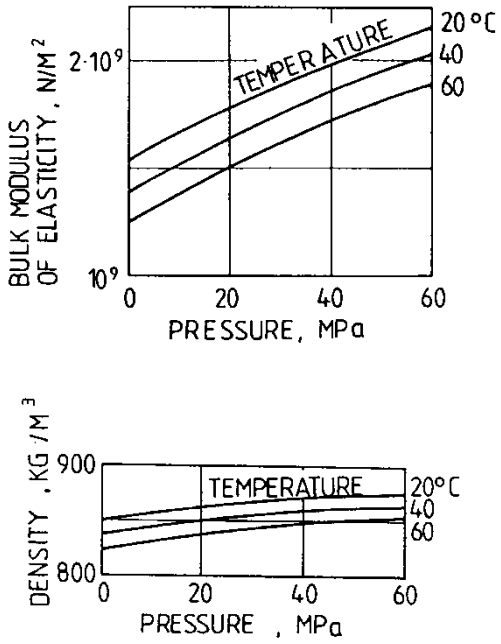

Figure 4: *Elastic module (above) and density (below) of fluid depending on pressure and temperature*

During the injection procedure, the pressure reaches 150 MPa; therefore, elastic modulus, E_{din}, of the fluid depends on pressure. The diagrams (Fig. 4) show that, in the first approximation, the elastic modulus and the specific density ρ evince linear dependence on the pressure, which is also taken into account in our computation.

Assumptions in a physical model:

1. All elastic deformations of the nozzle due to the change in pressure have been ignored.
2. Equations dealing with fluid ignore the fluid inertia.
3. Effective flow areas $\mu_s A_s$ and $\mu_l A_l$ (Fig. 2) were measured at steady flow as well as steady pressure, i.e. in rather ideal conditions compared with those prevailing during injection of fuel.

3 MATHEMATICAL MODEL OF THE DIESEL SPRAY

The mathematical model of the diesel spray presented here is based on continuity and momentum equations, which are in an Eulerian-Lagrangian formulation [5]. The spray is treated from fuel outlet of the nozzle to the mixture formation, ideal for self-ignition in the combustion chamber of the diesel engine. The fuel leaves the nozzle sac volume at high velocity due to pressure difference $p_{IV} - p_z$. p_z stands for combustion pressure.

The exit velocity of the fuel, u(t), is calculated on the basis of the injection characteristics, Q(t) (Fig.5):

$$u(t) = Q(t)/A \quad (3.1)$$

An injection characteristic is calculated with a computer simulation of the fuel injection system. Computer simulation of the spray cannot be carried out without previously calculated fuel injection parameters.

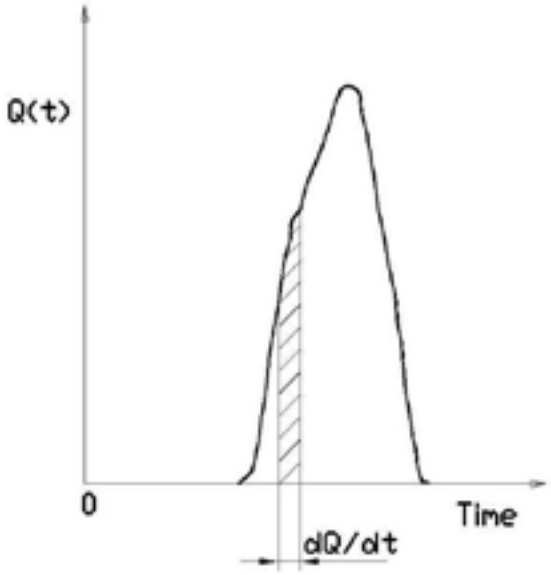

Figure 5: *Injection rate*

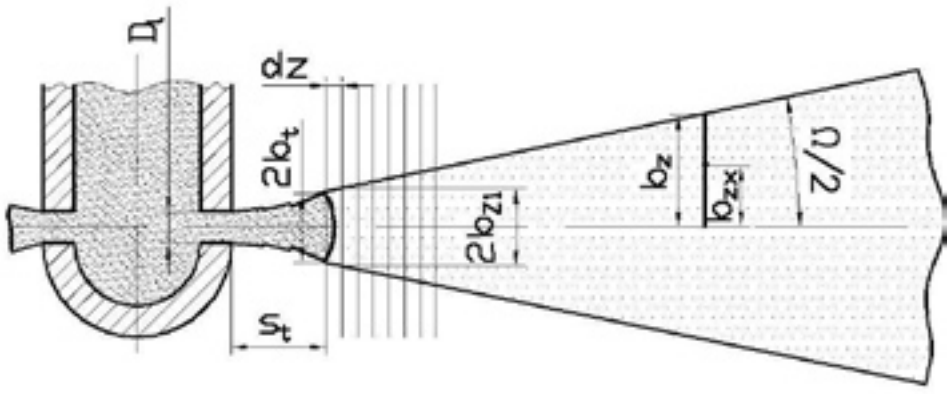

Figure 6: *Spray of the injected fuel*

At the exit of the nozzle, the fuel jet hits air and starts pushing it. At the beginning, the jet is in liquid phase, after a certain distance, s_t (Fig. 6), affected by external forces (aerodynamic force being the most important one), it breaks up into small droplets. The latter break up further into smaller droplets until the balance between the internal forces in droplets and external forces [1, 9, 10] is achieved. With a modern high pressure common rail fuel-injection system, the jet breaks up into droplets at the outlet of the nozzle due to strong turbulence and cavitation in the nozzle hole [6, 7, 8].

The following equations are applied in the mathematical model of the spray:

1. continuity equation for fuel

$$\frac{d}{dz}\left(u_z(t)\rho_g\right)=0 \tag{3.2}$$

2. continuity equation for fuel-air mixture

$$\frac{d}{dz}\left(\rho(t)u_z(t)\right)=\alpha 2\pi b(t)u_z(t)\left[\rho_m(t)\rho_a\right]^{0.5}\frac{1}{dA} \tag{3.3}$$

3. momentum equation for fuel-air mixture

$$\frac{d}{dz}\left(\rho(t)u_z(t)\right)\pm\frac{d}{dz}p_{din}=F_d\,, \tag{3.4}$$

where $\rho(t)$ and u (t) are local values. Local density $\rho(t)$ in any point of the spray is expressed as the function of the air density ρ_a in the spray and concentration C and density of the fuel ρ_g.

We introduced the following assumptions in the equations 3.2, 3.3 and 3.4:

1. All parameters required for spray description are treated as non-stationary.
2. The jet is treated as axisymmetrical in the x-y plane.
3. The jet is split into two parts: first, from the moment when the fuel exits from the nozzle and starts breaking up into droplets, and second from the moment of breaking up into droplets until their stagnation.

Local density in the equation 3.2, 3.3 and 3.4 is

$$\rho=\frac{\rho_a}{1-C\beta}\,, \tag{3.5}$$

where

$$\beta=1-\frac{\rho_a}{\rho_g}\,,\ C=\frac{m_g}{m}\,, m=m_g+m_a\,, \tag{3.6}$$

m_g is mass of fuel and m_a is mass of air.

Also introduced is the dimensionless factor ε, which demonstrates at a certain distance z from the injection nozzle the $\frac{b_{zx}}{b_z}$ relation, where b_z is the spray radius and b_{zx} is the spray local point distance.

$$\varepsilon = \frac{b_{zx}}{b_z} \tag{3.7}$$

Also introduced with this factor is the distribution function, $f(\varepsilon)$, which allows the calculation of the density, concentration and the speed profile in the spray. The distribution function is

$$f(\varepsilon) = 1 - \varepsilon^{1.5}, \tag{3.8}$$

density, concentration and the speed are

$$\rho = \rho_m f(\varepsilon), \qquad C = C_m f(\varepsilon) \text{and} \qquad u = u_m f(\varepsilon), \tag{3.9}$$

where index m stands for the middle of the spray.

In equations 3.2, 3.3 and 3.4 we insert equation 3.7, 3.8, 3.9 and obtain

1. continuity equation for fuel

$$\frac{d}{dz}\left(2\pi b^2 \rho_a u_m \int_0^1 \frac{C_m\left(1-\varepsilon^{1.5}\right)^3}{1-\beta C_m\left(1-\varepsilon^{1.5}\right)}\varepsilon d\varepsilon\right) = 0, \tag{3.10}$$

2. continuity equation for fuel-air mixture

$$\frac{d}{dz}\left(2\pi b^2 \rho_a u_m \int_0^1 \frac{\left(1-\varepsilon^{1.5}\right)^2}{1-\beta C_m\left(1-\varepsilon^{1.5}\right)}\varepsilon d\varepsilon\right) = \alpha 2\pi b u_m \left(\rho_g \rho_a\right)^{0.5} \tag{3.11}$$

where α stands for air entrainment coefficient.

3. momentum equation for fuel-air mixture

$$\begin{aligned} &\frac{d}{dz}\left(2\pi b^2 \rho_a u_m^2 \int_0^1 \frac{\left(1-\varepsilon^{1.5}\right)^4}{1-\beta C_m\left(1-\varepsilon^{1.5}\right)}\varepsilon d\varepsilon\right) \pm \\ &\frac{d}{dz}\left(2\pi b^2 \rho_a \frac{u_m^2}{2} \int_0^1 \frac{\left(1-\varepsilon^{1.5}\right)^2}{1-\beta C_m\left(1-\varepsilon^{1.5}\right)}\varepsilon d\varepsilon\right) = \pi b^2 C_d \rho_a \frac{u_m^2}{2} \end{aligned} \tag{3.12}$$

where C_d is air resistance coefficient.

Those equations apply to the second part of the spray, i.e. from the moment of breaking up into fine droplets until their stagnation (Fig. 6).

From continuity and momentum equations, we calculated diameter $2b_t$ of the liquid jet and point, s_t (Fig. 6)

The continuity equation for the fuel at the nozzle outlet hole and point, s_t, is

$$2\pi b_t^2 \rho_a u_0 \int_0^1 \frac{\left(1-\varepsilon^{1.5}\right)^3}{1-\beta c_m\left(1-\varepsilon^{1.5}\right)} \varepsilon d\varepsilon = \rho_g \frac{\pi D_l^2}{4} u_0 , \tag{3.13}$$

momentum equation for the fuel is

$$2\pi b_t^2 \rho_a u_0^2 \int_0^1 \frac{\left(1-\varepsilon^{1.5}\right)^4}{1-\beta c_m\left(1-\varepsilon^{1.5}\right)} \varepsilon d\varepsilon = \rho_g \frac{\pi D_l^2}{4} u_0^2 . \tag{3.14}$$

With equations 3.10, 3.11 and 3.12, we can compute the velocity and the diameter of the spray and fuel concentration in the spray. The equations are numerically solved by applying the Runge-Kutta method. The values constantly vary due to the velocity of the fuel exiting from the nozzle, which changes with time.

The computation is made by dividing injection characteristics into individual limit intervals (Fig. 5). The exit velocity, u, is computed for each such interval. The intervals are then further divided into small fuel elementary volumes (packages), exiting from the nozzle (Fig. 6). The same velocity is assumed within each of these volumes, whereas the velocity of a single volume differs from one volume to another. Each elementary volume consists of a large number of droplets. By applying known equations, their mean d_{mz}, maximum d_{maxz} and minimum d_{minz} diameters can be computed (3.5, 3.6, 3.7, 3.8, 3.9).

$$d_{mz} = 1.1\left[25+50\left(D_l-0.2\right)+30\left(1-\frac{p_{IV}}{300}\right)\left(\frac{150}{p_{IV}}\right)\left(\frac{l_b}{D_l}\right)^{\frac{1}{8}}\right], \tag{3.15}$$

$$d_{\min z} = \frac{0.25}{D_l+0.25}\left(\frac{p_{IV}}{300}\right)^{\frac{1}{4}}\left(\frac{l_b}{D_l}\right)^{\frac{1}{8}} d_m , \tag{3.16}$$

$$d_{\max z} = 2d_{mz} - d_{\min z} \tag{3.17}$$

where nozzle hole diameter, D_l, is in millimetres and sac pressure, p_{IV}, is in bars. The sac pressure is actually the injection pressure. These equations are applied for droplet diameters in the spray centre. Both theory [15] and practice show that bigger droplets are found in the middle of the spray, and the smaller ones at the edges. Therefore, diameters of droplets of elementary volumes found at the edges of the spray are computed with the equation

$$\begin{aligned} d_{mzx} &= d_{mz} f(\varepsilon), \\ d_{\min zx} &= d_{\min z} f(\varepsilon) \\ d_{\max zx} &= d_{\max z} f(\varepsilon). \end{aligned} \tag{3.18}$$

If the concentration and the mean diameter, d_m, of liquid droplets, in the moment of forming the spray at point, s_t, are known, their number in elementary volumes can be computed. By applying the law of droplet evaporation [1], vapour quantity in an elementary volume can be also computed. The law of droplet evaporation is

$$-\frac{d(d_m^2)}{dt} = \lambda \tag{3.19}$$

$$\lambda = \lambda_0\left(1 + 0.27\,\mathrm{Re}^{\frac{1}{2}}\,Sc^{\frac{1}{3}}\right)$$

$$\mathrm{Re} = \frac{u d_m}{\nu}$$

$$Sc = \frac{\nu}{D} = \frac{\eta}{\rho D}$$

$$\lambda_0 = \frac{8k_p}{\rho_g c_{pa}}\ln(1+B)$$

$$B = \frac{1}{L_u} c_{pa}\left(T_a - T_g\right)$$

In the equation 3.19, λ is the evaporation constant for forced convection, k_p is thermal conductivity, c_{pa} is the specific heat of surrounding air, L_u is latent heat of vaporization, T_a is temperature of surrounding air, T_g is temperature of droplet surface, Re is the Reynolds number, Sc is the Schmidt number, ν is kinematic viscosity, η is dynamic viscosity and D diffusivity.

The mass of the fuel m_g and air m_a is characterized by the equations

$$m = m_g + m_a\,, \tag{3.20}$$

$$m_g = Cm\,.$$

In the elementary volume, the fuel is in a liquid and vapour form. Fuel mass, m_g, is

$$m_g = m_{gl} + m_{gv}\,. \tag{3.21}$$

The number of droplets N in the elementary volume on the distance, s_t, is

$$N = \frac{6m_g}{\pi d_m^3 \rho_g}\,. \tag{3.22}$$

The mass of vapour fuel, m_{gv}, in elementary volume is

$$m_{gv} = \frac{\pi}{6}\rho_g\left[d_m^3 - \left(d_m - \frac{d\left(d_m^2\right)}{dt}\right)^3\right]N\,. \tag{3.23}$$

The mass of liquid fuel, m_{gl}, in elementary volume is

$$m_{gl} = \frac{\pi d_m^3}{6} \rho_g N . \tag{3.24}$$

The conditions in the diesel engine combustion chamber continuously change due to varying engine rpm and engine load. For good combustion process control, it is necessary to know the point at which combustion self-ignition occurs. A new criterion for determining the self-ignition nuclei, based on assumptions that the strongest combustion self-ignition probability lies in those elementary volumes, in which the stoichiometric air ratio is and the fuel is evaporated or fuel droplet diameter is equal or lower than 0.0065 mm. The most efficient combustion with regard to the consumption and emission will be in those points or elementary volumes containing the stoichiometric air ratio and the fuel droplets with the lowest mean diameters.

In order to determine the points or elementary volumes in which self-ignition occurs first, we have introduced the term "ignition probability Ψ" referring to the local air ratio and fuel dispersion quality in the spray. The ignition probability Ψ is

$$\Psi = \Psi_c \Psi_d \leq 1 . \tag{3.25}$$

The term Ψ_c takes into account the local air ratio in the spray and has the highest value for stoichiometric air ratio.

$$\mathrm{Y}_c = \exp\left[-\left| \ln \frac{\varphi_r}{\varphi_s} \right| \right]$$

$$\varphi_r = \frac{m_g}{m_a} \quad \varphi_s = \frac{m_g}{m_a} = 0.071 \tag{3.26}$$

The term Ψ_d takes into account the fuel spray dispersion quality and has the maximum value at droplet diameters d_{opt} = 0.0065 mm or less. The droplets with diameters of 0.0065 mm may already be treated as those burning as gas.

$$\Psi_d = \frac{1}{3\sigma_0 (2\pi)^{\frac{1}{2}}} \exp\left[-\frac{1}{2} \left(\frac{d_m - d_{opt}}{3\sigma_0} \right)^2 \right] \tag{3.27}$$

$$\sigma_0 = \left| d_m - d_{\min} \right|$$

The points where Ψ has equal value are joined into curves so as to obtain the areas where the probability of self-ignition is the strongest (Fig. 17).

---

4 COMPUTER SIMULATION

All data concerning nozzles obtained partly from technical documentation and partly by measuring are stored in a database so as to ensure an easily accessible source of information available at any time. Programs required for simulation of common rail and diesel spray can be developed by combining different programs for the simulation of the fuel injection system. We developed a computer simulation of various classical and common rail injection systems [18, 19].

All mathematical models of the nozzle are solved numerically according to the Runge-Kutta method of the fourth order, by means of the changeable integration step. The integration step changes during the operation, depending on the initial step of integration as well as on permissible errors and factual errors of integration. As soon as the factual error exceeds the permissible error, the step is halved. The program allows a ten-fold halving of the integration step. In cases processed during our investigation, the error did not exceed a pressure of 0,1 bar when the timing prescribed for the initial step of integration ranged between 10 and 20 μ sec. (0.06-0.12 of crank angle degree at 1000 r.p.m.).

The input data for the injection parameter and spray computation is the pressure in a high-pressure accumulator (rail) (Fig. 11) and the electric current at the triggering element (solenoid valve) (Fig. 10). Those data were recorded on a magnetic tape and then stored in the computer memory via an analogous digital converter. The programs run on a PC or on an ALPHA DS-20 computer.

We developed several computer programs for classical and common rail fuel injection systems; therefore, various combinations of injection system-spray programs can be used. The combination of programs depends on engine equipment.

5 OPTICALLY ACCESSIBLE ENGINE

Fig. 7 shows the transparent engine used in this study. The engine is a single-cylinder transparent engine based on the AUDI V6 TDI engine. Construction details have been discussed in other publications [16, 17] and Table 1. In contrast to former investigations, the diameter of the flat bottom piston bowl was increased from 40 mm to 48 mm. The compression ratio of 15.5 was kept constant. The difference to the serial engine (19.5) was compensated with an external heatable intake air charging, which guaranteed identical cylinder pressures in TDC.

The engine is equipped with a Bosch common rail injection system, which can deliver pressures up to 1350 bar. Two 6-hole mini-sac-hole nozzles were investigated, which differ significantly in their flow values (μ = 0.77 / μ= 0.62). The flow value is a function of the conicity and the hydro grinding of the injections holes, and regards the relationship between ideal and actual streaming. Here, different flow values describe different momentums of the injected fuel (high value: fast injection). The injected fuel volume is 12 mm^3 for every operating point.

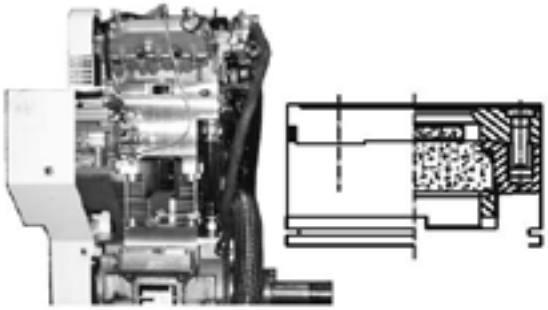

Figure 7: *Optically accessible engine with piston crown (based on AUDI V6 TDI)*

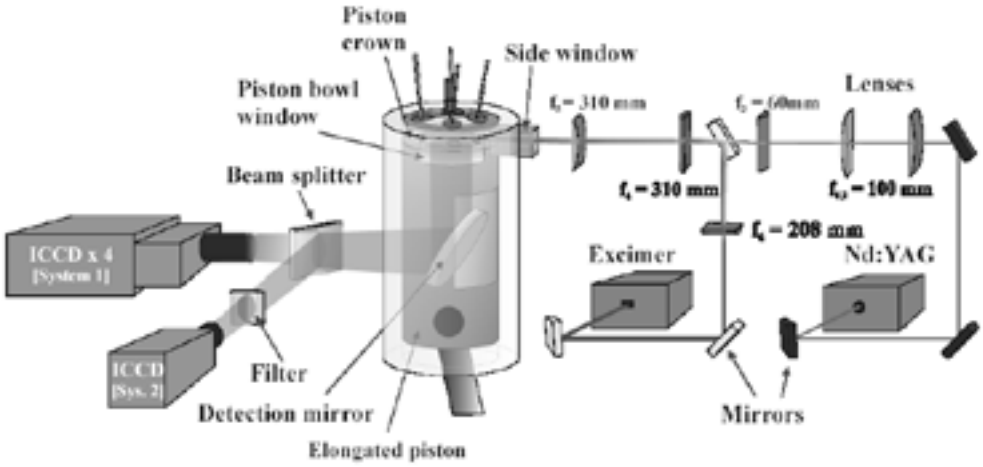

Figure 8: *Optical set-up*

The nozzles were compared at a rail pressure of 1350 bar. Additionally, the rail pressure was decreased to 800 bar, using the nozzle with μ = 0.77. The influence of a pre-injection was investigated at a rail pressure of 800 bar (μ = 0.77). All investigations were carried out at an engine speed of 1500 rpm and a non-fired cylinder pressure, p_z, of 55 bar.

6 MEASUREMENT TECHNIQUE

The optical part of the experimental set-up and the transparent engine is outlined in Fig. 8. The combination of two different lasers and camera systems allows the simultaneous detection of the Mie scattering of the injected fuel, the laser-induced fluorescence of fuel and vapour, the premixed combustion mode and the diffusion mode.

For the detection of the diffusion flame, which delivers significant emission intensities in the visible range of the light, an enhanced CCD camera was used. It is placed in a housing, which can contain up to four cameras that are individually triggered (System 1). The exposure time of the first camera is 1 μs.

The detection of the premixed flame, which delivers significant emission intensities in the UV range, is realised by the application of a separate intensified UV camera (System 2), placed

---

perpendicularly to the first camera. Due to the transmission character of the filters used and the beam splitter, only wavelengths in the range of 300 nm to 380 nm are detected by this camera. Its exposure time is also 1 µs.

An excimer laser (wavelength: 248 nm, pulse duration: 20 ns) excites the fuel and vapour to fluorescence with strong intensities in the UV range. Because the UV camera (System 2) is equipped with a double shutter function, it is possible to detect the laser-induced fluorescence with a second exposure. As the exposure time is only 140 ns, no influences of the premixed flame can be seen.

A Nd:YAG laser is used for the excitation of Mie scattering at a wavelength of 532 nm (pulse duration: 10 ns) to detect the injection with a second intensified camera, placed in the housing of the intensified CCD camera (System 1). A filter is applied to suppress influences of the combustion signal. The exposure time is 200 ns. For an easier and better understanding, the engine and optical timing is shown in Fig. 9.

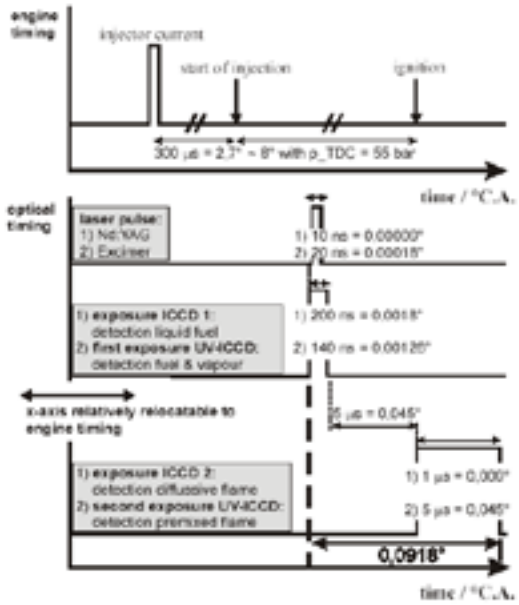

Figure 9: *Engine and optical timing*

Table 1: *Engine data*

Stroke	86.4 mm
Bore	78.3 mm
s/d (stroke / bore)	1.1
Displacement	0.416 litre
r/l (crank radius / conrod length)	0.273
Compression ratio (serial)	19.5
Compression ratio	15.5
Combustion bowl (depth)	10.55 mm
Combustion bowl (Ø)	48 mm
Swirl level (Tippelmann)	0.49

7 COMPARISON OF MEASURED AND CALCULATED VALUES

This chapter contains the results of the injection system, spray and combustion simulation, measurements in an optically accessible engine and the comparison between the computed and measured parameters. All measurements were carried out in single-cylinder transparent engine based on the AUDI V6 engine, equipped with a Bosch common rail injection system. We used Bosch DLLA 6 HD 360 6-holes mini-sac-hole nozzle with the flow value $\mu = 0.77$.

The injection process, spray and ignition at 1500 rpm of the engine and p_{rail}=800 bar are simulated. Input data are for the computer simulation of the injection process, spray and ignition are cylinder pressure, injector current and rail pressure. Figure 10 shows the cylinder pressure and electric current. In Figures 11 to 14, the calculated pressure, p_{IV}, in sac volume, needle lift, h_i, injection rate and total injected fuel are shown. We simulated and measured a two-stage injection process. The calculated pre-injected amount of the fuel was 0.94 mm^3 and the measured amount 0.779 mm^3. The calculated main-injected amount of the fuel was 11.85 mm^3 and the measured amount 11.97 mm^3. The congruity between the calculated and measured data is excellent. Figure 11 shows that pressure, p_{IV}, is much lower for pre-injection than for main injection, because the injection rate for pre-injection is twelve times smaller than for main injection. Low pressure, p_{IV}, means a greater Sauter diameter of fuel droplets and worse fuel distribution. Measurement of pressure, p_{IV}, in the sac volume is very demanding. Computer simulation, in that case, enables in-depth view of the injection process.

The input data for spray simulation is the injection rate (Fig. 5, 13) and pressure, p_{IV}, which are decisive for the spray formation. Figure 18 shows the liquid phase of the spray, which is detected by Mie scattering of the light. The measured spray cone is 7.1 degrees and the simulated one is 7.21 degrees. The congruity between the calculated and measured data is again excellent.

Figure 15 shows a total air ratio λ_{tot} in the spray, whereas Figure 16 shows air ratio λ_v, where only fuel vapour is taken into account. More important for the calculation of the probability of mixture self-ignition is the air ratio, with solely the fuel vapour being taken into account. The comparison of Fig. 15 and 16 shows that the areas where $\lambda_{tot} = \lambda_v = 1$ do not fully

---

overlap. The greatest areas $\lambda_{tot} = 1$ are at the end and close to the edge of the spray. A little area $\lambda_{tot} = 1$ also lies at the last quarter and very close to the spray axis. Very small areas with $\lambda_{tot} = 1$ and very close to $\lambda_{tot} = 1$ also lie at the edge of the spray and close to the tip of the nozzle. The areas with $\lambda_v = 1$ are greater than areas with $\lambda_{tot} = 1$. The greatest area with $\lambda_v = 1$ spreads from the middle of the spray axis, then runs between the edge and axis of the spray to his end. Small areas where $\lambda_v = 1$ are at the edge and close to the tip of the nozzle.

Fig. 17 shows the areas of probability of the spray mixture self-ignition. The greatest area with the highest calculated probability of the mixture self-ignition is in the last half and outside the spray axis. A small area with the highest probability also lies near the nozzle and at the edge of the spray. At the edge of the spray, seven millimetres from the tip of the nozzle lies a small area with high probability of the mixture self-ignition.

Simulation results show that spray contains areas with very high and very low values of air ratio λ, which is the consequence of very strong turbulence in the spray. The structure of the spray is very heterogeneous.

Fig. 19 shows spray formation and premixed combustion. The liquid phase of the spray is detected by the application of the Mie scattering technique, the liquid and vapour phase by laser-induced fluorescence (LIF) technique. The pre-injection starts at seven degrees before TDC (Fig. 19). The vaporisation is nearly finished at 5 degrees before TDC. There is no evidence of self-ignition after finished vaporisation of pre-injected spray. The main injection starts nearly at four degrees before TDC and is completed at TDC.

The first evidence of the self-ignition is at TDC (Fig. 19), which is in accordance with in-cylinder pressure diagram (Fig. 10). Four of the six sprays ignite at the end and close to the edge of the spray where the greatest area of the highest calculated probability of self-ignition is (Fig. 17). Self-ignition also occurs at the small areas of the highest calculated probability of self-ignition in the vicinity of the nozzle tip. The agreement between the calculated areas of self-ignition and the measured one is relatively good. After self-ignition, the premixed flame burns from outer regions of the combustion chamber to inner region in direction to the nozzle tip.

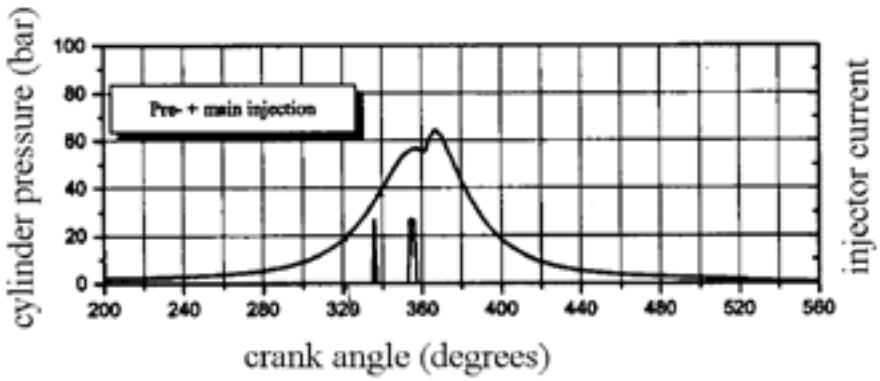

Figure 10: *Cylinder pressure and injector current (n= 1500 rpm, p_{rail}=800 bar)*

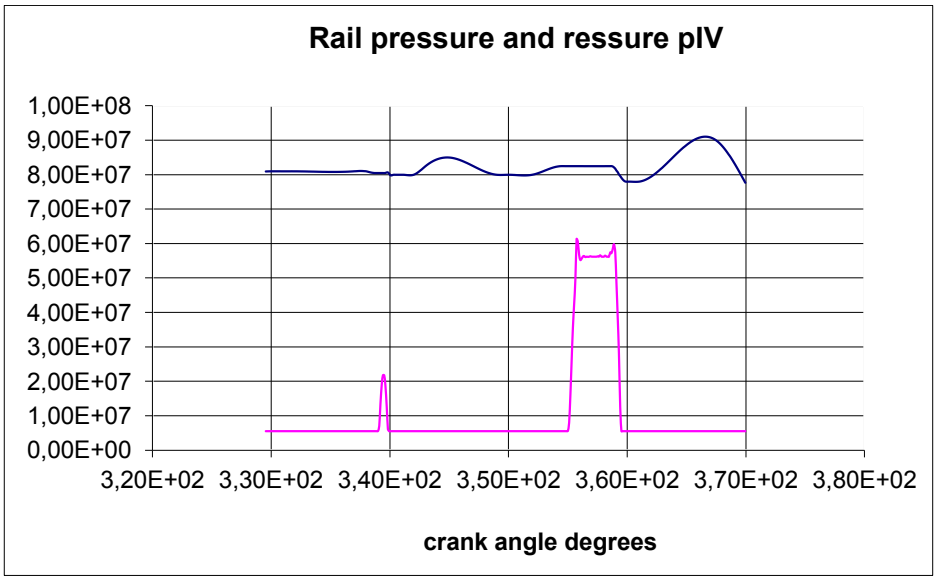

Figure 11: *Measured rail pressure and calculated pressure* p_{IV}

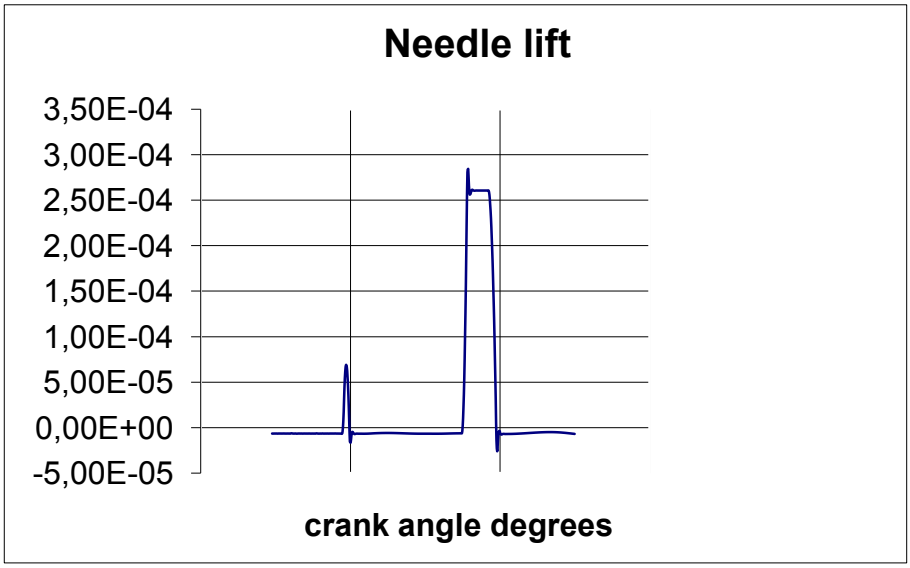

Figure 12: *Needle lift*

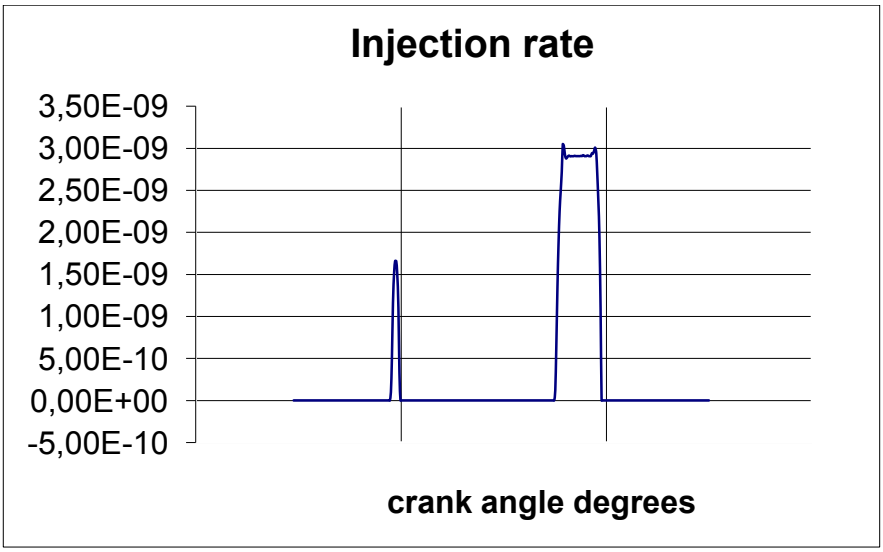

Figure 13: *Injection rate*

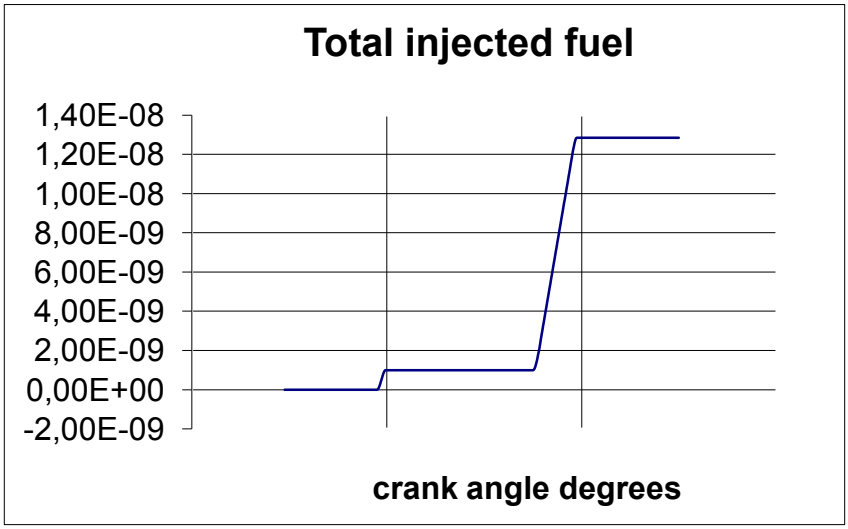

Figure 14: *Total injected fuel*

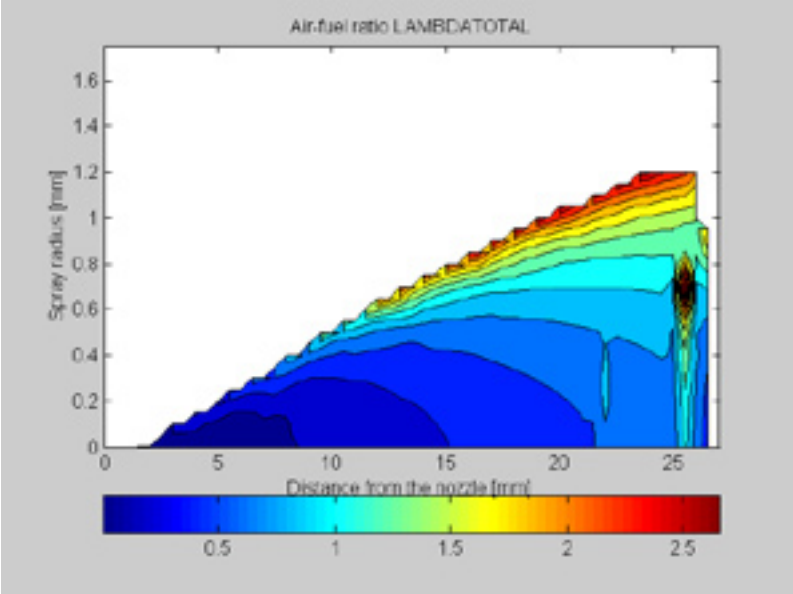

Figure 15: *Total air-fuel ratio*

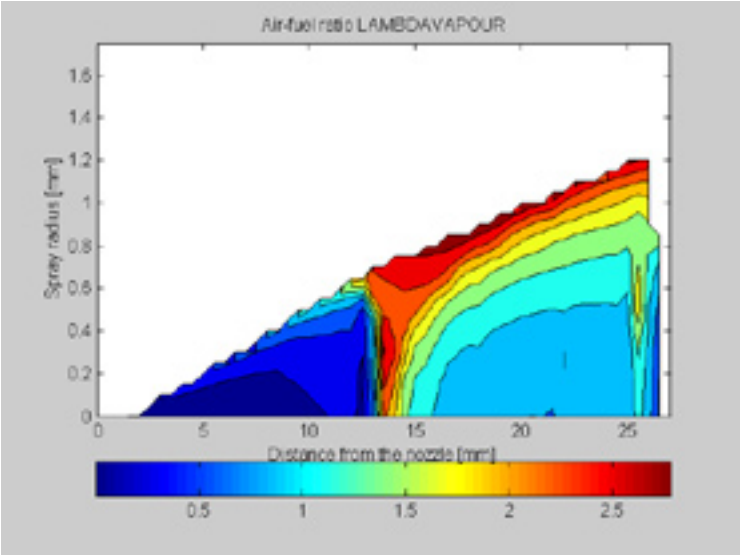

Figure 16: *Air-fuel vapour ratio*

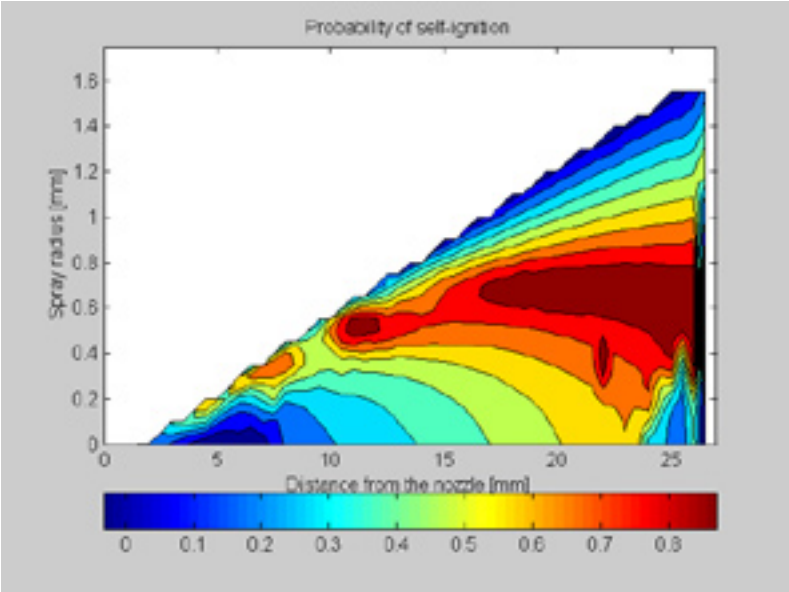

Figure 17: *Probability of self-ignition*

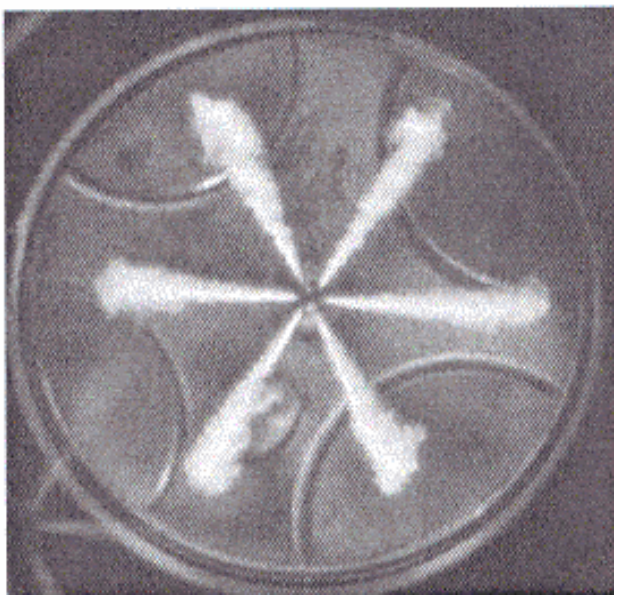

Figure 18: *Spray formation*

Mie scattering **LIF**

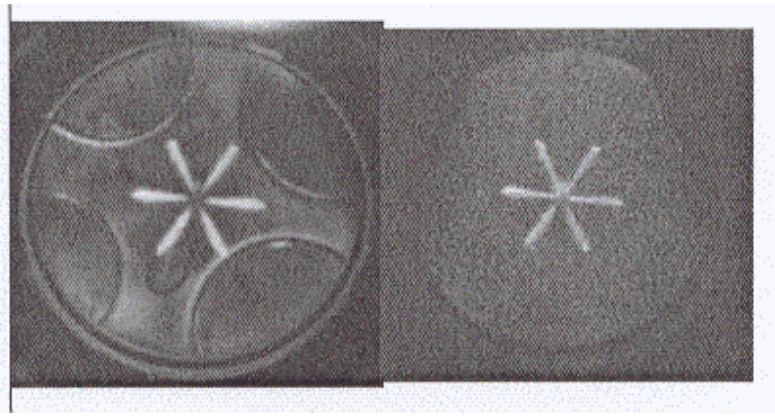

7degrees before TDC

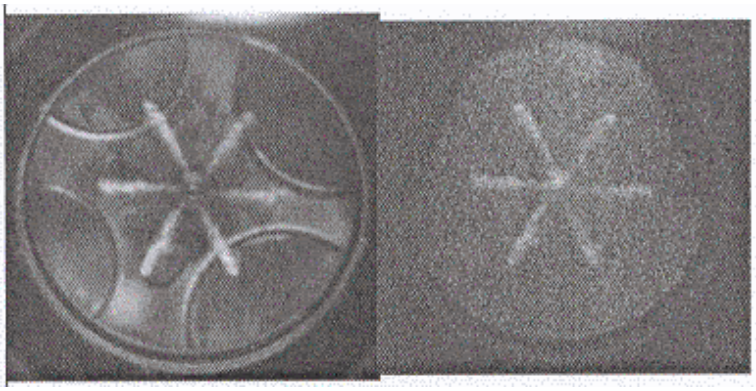

6 degrees before TDC

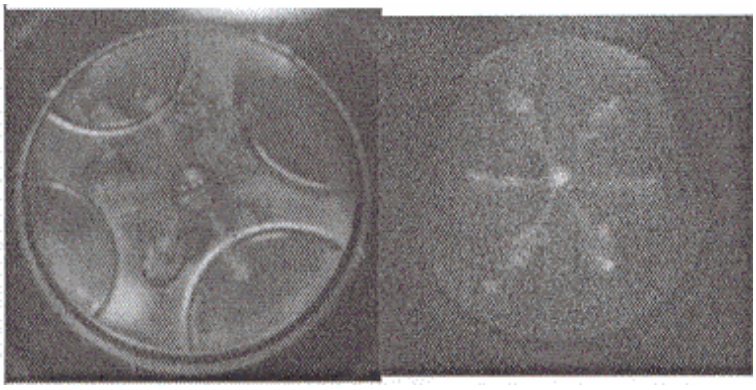

5 degrees before TDC

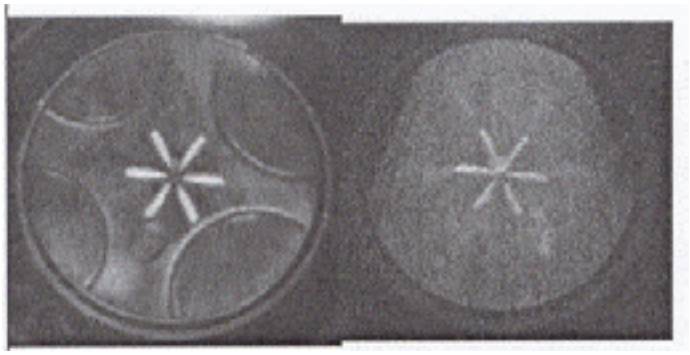

4 degrees before TDC

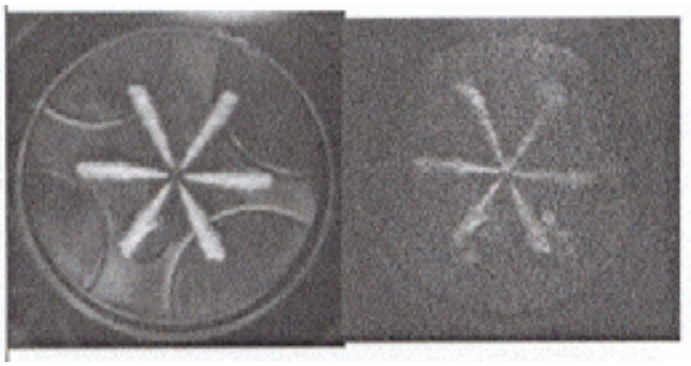

3 degrees before TDC

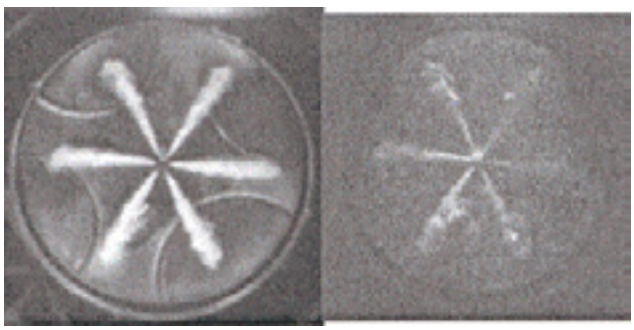

2 degrees before TDC

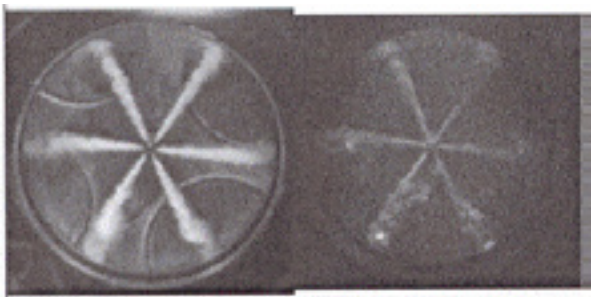

1 degrees before TDC

Mie scattering **LIF** **Premixed combustion**

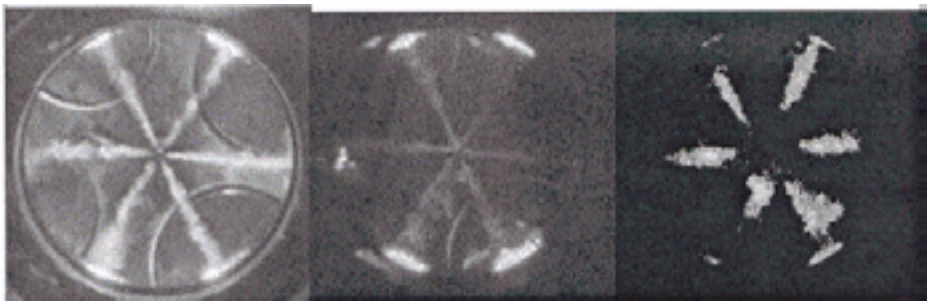

Top Dead Centre

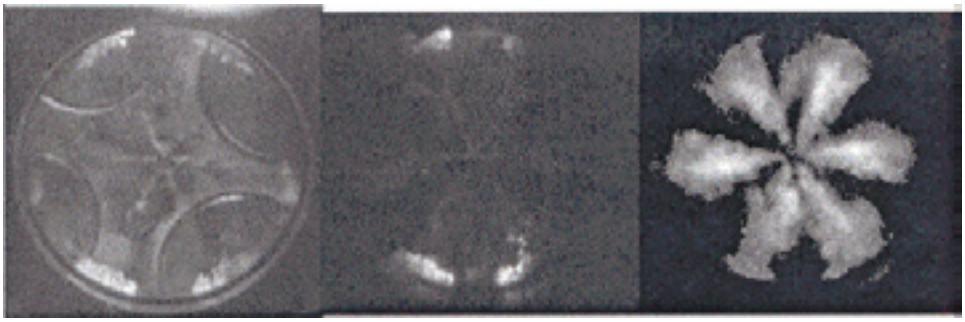

1 degrees after TDC

Figure 19: *Spray formation and combustion process (n=1500 rpm, p_{rail}=800 bar)*

8 CONCLUSIONS

This paper describes a computer simulation of the common rail accumulator fuel-injection system and the diesel spray. The injection system simulation results constitute the input data

---

for the spray calculation. Both programs are structurally separated, thus allowing their utilisation for various injection systems and the spray program.

The input data for the injection system simulation comprises the injector current and rail pressure. The computer simulation allows the calculation of the following injection parameters:

1. Pressure p_{IV} in the sac volume.
2. Acceleration, velocity and lift of the needle.
3. Injection rate.
4. Total amount of the injected fuel.

The comparison of the computed and measured total amount of the injected fuel showed excellent agreement.

The spray simulation is based upon the continuity and momentum equation. The entire spray is divided into small volumes, in which the minimum, mean and maximum droplet diameters are calculated as well as the quantity of air and liquid and the evaporated fuel. Moreover, the number of droplets and the total air-fuel ratio and air-fuel vapour ratio are calculated in each volume. A new criterion for the calculation of the mixture self-ignition is defined here, based upon the assumption that with regard to consumption and pollution, combustion is most efficient in elementary volumes with a stoichiometric air ratio. The second assumption refers to the fuel dispersion quality, i.e. that droplets with diameters of less than 0.0065 mm burn practically as fuel vapour. These two assumptions are used to compute the highest probability of the mixture self-ignition. The elementary volumes with the same self-ignition probabilities are then joined by a curve to obtain the areas of identical mixture self-ignition probabilities.

The experiments were carried out in a single-cylinder transparent engine, based on the Audi V6 TDI engine. The engine is equipped with a Bosch common rail injection system and a 6-hole mini-sac-hole nozzle. The optical part of the experimental set-up contains a combination of two different lasers and camera systems, which allows the simultaneous detection of the Mie scattering of the injected fuel, the laser-induced fluorescence of fuel and vapour, the premixed combustion mode and the diffusion mode.

The comparison of the calculated and measured amount of the injected fuel shows excellent agreement. The calculated main-injected amount of the fuel was 11.85 mm^3 and the measured amount 11.97 mm^3.

The agreement between the calculated and measured spray cone is excellent; the measured spray cone is 7.1 degrees and the simulated one is 7.21 degrees.

The self-ignition of the combustible mixture occurs at the end and close to the edge of the spray. Self-ignition also occurs in the vicinity of the nozzle tip. The agreement between measured and calculated points of self-ignition is relatively good, thus confirming our theory of self-ignition.

The impacts of various structural elements of the injection system on the injection and spray formation process can be very quickly assessed through a computer simulation, which results in much less expensive experiments.

References

[1] **N. A. Chieger**: *Energy and Combustion Science*, Pergamon Press, U. K., 1979

[2] **L. Allevi**: *Algemeine Theorie über der veränderliche Bewegung das Wasser in Leitungen*, Springer Verlag, Berlin, 1909

[3] **A. M. Rothrock**: *Hydraulics of Fuel Injection Pump for Compression-Ignition Engines*, NACA Report No. 396

[4] **W. Schley**: *Teoretische und experimentelle Untersuchungen zur analytischen Darstellung der Wellendämpfungen von hydraulischen Einspritzsystemen*, Diss. München, 1967

[5] **M. Gorokhovski**: *The Stochastic Lagrangian Model of Drop Breakup in the Computation of Liquid Sprays*, Atomization and Sprays, vol. 11, pp.505–519, 2001

[6] **N. Levy, S. Amara and J.-C. Champoussin**: *Simulation of a Diesel Jet Assumed Fully Atomized at the Nozzle Exit*, SAE 981067

[7] **C. Heimgärtner, A. Leipertz**: *Investigation of Primary Diesel Spray Break-up Close to Nozzle of a Common-Rail High Pressure Injection System*, SAE 2000-01-1799

[8] **A. Fath, C. Fettes, A. Leipertz**: *Investigation of the Diesel Spray Break-up Close to the Nozzle at Different Injection Conditions*, Proc. COMODIA 98, Kyoto, Japan, July 1998, pp. 429–434

[9] **J. V. Sinnamon, A. Lancaster, I. C. Steiner**: *An Experimental and Analitical Study of Engine Fuel Spray Trajectories*, SAE 800135

[10] **G. N. Abramowich**: *The Theory of Turbulent Jets*, MIT Press, Cambridge, Massachusetts

[11] **H. Hiroyasu, F. Nishida**: *Simplified Three-Dimensional Modelling of Mixture Formation and Combustionin in a D. I. Diesel Engine*, SAE 890269

[12] **K. S. Varde, D. M. Papa**: *Spray Angle and Atomization in Diesel Sprays*, SAE 841055

[13] **T. Kamimoto, S. K. Ahn, M. Chan**: *Measurement of Droplet Diameter and Fuel Concentration in a Non-Evaporating Diesel Spray By Means of an Image Analysis of Shadow Photographs*, SAE 840274

[14] **M. Arai, M. Tabata, H. Hiroyasu, M. Shimizu**: *Disintegrating Process and Spray Characterization of Fuel Jet Injected by a Diesel Nozzle*, SAE 840275

[15] **T. Takeuchi, H. Hiroyasu, J. Senda, K. Yamada**: *Droplet Size Distribution in Diesel Fuel Spray*, JSME 26, No. 215, May 1983

[16] **C. Fettes, S. Schraml, C. Heimgärtner, A. Leipertz**: *Analysis of the Combustion Process in a Transparent Passenger Car DI-Diesel Engine by Means of Multi-Dimensional Optical Measurements Techniques*, SAE 2000-01-2860 (2000)

[17] **C. Fettes, A. Leipertz**: *Potentials of a Piezo-Driven Passenger Car Common Rail System to Meet Future Emission Legislations-An Evaluationby Means of In-Cylinder Analysis of Injection and Combustion*, SAE 2001-01-3499 (2001)

[18] **M. Marcic, Z. Kovacic**: *Computer Simulation of the Diesel Fuel Injection System*, SAE 851583 (1985)

[19] **M. Marcic**: *Calculation of the Diesel Fuel Injection Parameters*, SAE 952071 (1995)

---

http://www.fe.uni-mb.si/si/jet.html

AUTHOR INSTRUCTIONS (MAIN TITLE)

SLOVENIAN TITLE

Authors, Corresponding author[ℜ]

Key words: (Up to 10 keywords)

Abstract

Abstract should be up to 500 words long, with no pictures, photos, equations, tables, only text.

Povzetek

(In Slovenian language)

Submission of Manuscripts: All manuscripts must be submitted in English by e-mail to the editorial office at jet@uni-mb.si to ensure fast processing. Instructions for authors are also available online at www.fe.uni-mb.si/si/jet.html.

Preparation of manuscripts: Manuscripts must be typed in English in prescribed journal form (Word editor). A Word template is available at the Journal Home page.

A title page consists of the main title in the English and Slovenian languages; the author(s) name(s) as well as the address, affiliation, E-mail address, telephone and fax numbers of author(s). Corresponding author must be indicated.

Main title: should be centred and written with capital letters (ARIAL **bold** 18 pt), in first paragraph in English language, in second paragraph in Slovenian language.

Key words: A list of 3 up to 6 key words is essential for indexing purposes. (CALIBRI 10pt)

Abstract: Abstract should be up to 500 words long, with no pictures, photos, equations, tables, - text only.

Povzetek: - Abstract in Slovenian language.

[ℜ] Corresponding author and other authors: Title, Name and Surname, Tel.: +XXX x xxx xxx, Fax: +XXX x xxx xxx, Mailing address: xxxxxxxxxxxxxxxxxxxxxxxxxxxxxxxxx, E-mail address: email@xxx.xx

---

Main text should be structured logically in chapters, sections and sub-sections. Type of letters is Calibri, 10pt, full justified.

Units and abbreviations: Required are SI units. Abbreviations must be given in text when firstl mentioned.

Proofreading: The proof will be send by e-mail to the corresponding author, who is required to make their proof corrections on a print-out of the article in pdf format. The corresponding author is responsible to introduce corrections of data in the paper. The Editors are not responsible for damage or loss of manuscripts submitted. Contributors are advised to keep copies of their manuscript, illustrations and all other materials.

The statements, opinions and data contained in this publication are solely those of the individual authors and not of the publisher and the Editors. Neither the publisher nor the Editors can accept any legal responsibility for errors that could appear during the process.

Chapter examples:

1 MAIN CHAPTER

(Arial bold, 12pt, after paragraph 6pt space)

1.1 Section

(Arial bold, 11pt, after paragraph 6pt space)

1.1.1 Sub-section

(Arial bold, 10pt, after paragraph 6pt space)

Example of Equation (lined 2 cm from left margin, equation number in normal brackets (section.equation number), lined right margin, paragraph space 6pt before in after line):

$$c = \sqrt{a^2 + b^2} \tag{1.1}$$

Tables should have a legend that includes the title of the table at the top of the table. Each table should be cited in the text.

Table legend example:

Table 1: *Name of the table (centred, on top of the table)*

Figures and images should be labelled sequentially numbered (Arabic numbers) and cited in the text – Fig.1 or Figure 1. The legend should be below the image, picture, photo or drawing.

Figure legend example:

Figure 1: *Name of the figure (centred, on bottom of image, photo, or drawing)*

References

[1] **Name. Surname:** *Title,* Publisher, p.p., Year of Publication

Example of reference-1 citation: In text, Predin, [1], text continue. **(Reference number order!)**

SiPRO INŽENIRING

GEN ENERGIJA

JET

JET Journal of ENERGY TECHNOLOGY Vol. 5/1 2012 UNIVERSITY OF MARIBOR, FACULTY OF ENERGY TECHNOLOGY

9 771855 574008

ISSN 1855-5748